https://doi.org/10.5194/egusphere-2024-2602
Preprint. Discussion started: 7 October 2024

The Critical Role of Aqueous-Phase Processes in Aromatic-Derived Nitrogen-Containing Organic Aerosol Formation in Cities with Different Energy Consumption Patterns

Yi-Jia Ma[1,2,3], Yu Xu[2,3]*, Ting Yang[1,2,3], Lin Gui[1,2,3], Hong-Wei Xiao[2,3], Hao Xiao[2,3], and Hua-Yun Xiao[2,3]

[1]School of Environmental Science and Engineering, Shanghai Jiao Tong University, Shanghai 200240, China

[2]School of Agriculture and Biology, Shanghai Jiao Tong University, Shanghai 200240, China

[3]Shanghai Yangtze River Delta Eco-Environmental Change and Management Observation and Research Station, Ministry of Science and Technology, Ministry of Education, Shanghai 200240, China

Yu Xu (E-mail: xuyu360@sjtu.edu.cn)

+8615885507087

Shanghai Jiao Tong University, 800 Dongchuan Road

https://doi.org/10.5194/egusphere-2024-2602
Preprint. Discussion started: 7 October 2024

Abstract. Nitrogen-containing organic compounds (NOCs) impact air quality and human health. Here, the abundance, potential precursors, and main formation mechanisms of NOCs in $PM_{2.5}$ during winter were compared for the first time among Haerbin (coal-dependent for heating), Beijing (natural gas and coal as heating energy), and Hangzhou (no centralized heating policy). The total signal intensity of CHON+, CHN+, and CHON− compounds was highest in Haerbin and lowest in Hangzhou. Anthropogenic aromatics accounted for 73%–93% of all identified precursors of CHON+, CHN+, and CHON− compounds in Haerbin. Although the abundance of aromatics-derived NOCs was lower in Beijing than in Haerbin, aromatics were also the main contributors to NOC formation in Beijing. Hangzhou exhibited the lowest levels of aromatic precursors. Furthermore, non-metric multidimensional scaling analysis indicated an overall reduction in the impact of fossil fuel combustion on NOC pollution along the route from Haerbin to Beijing to Hangzhou. We found that aqueous-phase processes (mainly condensation, hydrolysis or dehydration processes for reduced NOCs, and mainly oxidization or hydrolysis processes for oxidized NOCs) can promote the transformation of precursors to produce NOCs, leading to the most significant increase in aromatic NOC levels in Haerbin (particularly on haze days). Reduced precursor emissions in Beijing and Hangzhou (the lowest) constrained the aqueous-phase formation of NOCs. The overall results suggest that the aerosol NOC pollution in coal-dependent cities is mainly controlled by anthropogenic aromatics

https://doi.org/10.5194/egusphere-2024-2602
Preprint. Discussion started: 7 October 2024

and aqueous-phase processes. Thus, without effective emission controls, the formation of NOCs through aqueous-phase processes may still pose a large threat to air quality.

Keywords: Aerosols, Nitrogen-containing organic compounds, Heating energy consumption, Anthropogenic pollutants, Formation mechanism

https://doi.org/10.5194/egusphere-2024-2602
Preprint. Discussion started: 7 October 2024

1. Introduction

Nitrogen-containing organic compounds (NOCs) are abundant reactive nitrogen species in aerosol particles, accounting for up to 40%–80% of total nitrogen deposition (Li et al., 2023; Xi et al., 2023; Yu et al., 2020). Clearly, aerosol NOCs can significantly contribute to the global nitrogen cycle (Li et al., 2023; Cape et al., 2011). Moreover, the formation of secondary organic aerosols (SOA) and light-absorbing organic aerosols (e.g., brown carbon) is also tightly associated with NOCs (Wang et al., 2024; Liu et al., 2023b; Zeng et al., 2021), thus affecting the radiative balance and air quality (Yuan et al., 2023; Jiang et al., 2023). In particular, certain NOCs, such as nitroaromatics and peroxyacyl nitrates, are characterized as phytotoxins and potential carcinogens, posing threats to ecosystems and human health (Shi et al., 2023; Singh and Kumar, 2022; Huang et al., 2024). Therefore, understanding the characteristics, origins, and atmospheric processes of NOCs is essential for comprehending their climate and health effects.

Aerosol NOCs can be derived from primary emissions associated with anthropogenic activities and natural sources (Cape et al., 2011; Lin et al., 2023; Xu et al., 2020a; Wang et al., 2017; Song et al., 2018; Song et al., 2022; Ma et al., 2024). Secondary formation processes may play a more crucial role in the formation of NOCs in fine aerosol particles, which involve interactions among volatile organic compounds (VOCs), atmospheric oxidants, and reactive inorganic nitrogen species

https://doi.org/10.5194/egusphere-2024-2602
Preprint. Discussion started: 7 October 2024

(Montoya-Aguilera et al., 2018; Perraud et al., 2012; Hallquist et al., 2009). For instance, laboratory studies have observed the formation of organic nitrates from the oxidation of isoprene and α-/β-pinene by atmospheric oxidants and nitrogen oxide (NO_x) (Surratt et al., 2010; Rollins et al., 2012; Nguyen et al., 2015). Additionally, aqueous-phase reactions of NH_4^+ (or NH_3) with biogenic VOCs or carbonyl compounds have been suggested to be important mechanisms of reduced NOC (Re-NOCs) formation (Abudumutailifu et al., 2024; Laskin et al., 2014; Li et al., 2019b; Liu et al., 2023b; Wang et al., 2024). However, understanding the origins, formation mechanisms, and environmental impacts of NOCs is hindered by the elusive and intractable molecular information regarding NOCs and their precursors.

Aerosol liquid water (ALW) can greatly increase the formation of aerosol NOCs by facilitating the conversion of water-soluble organic gases into particles and subsequently enabling aqueous-phase reactions (Li et al., 2019a; Lv et al., 2022; Liu et al., 2023b). A positive correlation between aerosol NOC abundance and either ALW or relative humidity (RH) has been observed in several observation studies (Jiang et al., 2023; Liu et al., 2023b; Xu et al., 2020b). In particular, it has been suggested that increased ALW levels can exacerbate winter haze in China (Wu et al., 2018; Hodas et al., 2014; Lv et al., 2022; Wang et al., 2021d; Liu et al., 2023b; Wang et al., 2021a; Li et al., 2019a). Presumably, precursors and ALW are the two key factors in the formation of aerosol NOCs. Haze environments have potentially high RH levels and

https://doi.org/10.5194/egusphere-2024-2602
Preprint. Discussion started: 7 October 2024

large emissions of NOC precursors. Moreover, in Chinese cities with different energy consumption (e.g., coal, biomass, and natural gas) for winter heating (Zhang et al., 2021b; Zhang et al., 2023b), the types and emission intensities of pollutants released from different heating sources are expected to vary considerably (Bond et al., 2006; Stockwell et al., 2015; Křůmal et al., 2019). However, the potential effects of ALW in the formation of NOCs in Chinese cities with different energy consumption during winter, particularly in haze periods, are not well documented. Moreover, the roles of ALW-related NOC formation processes in the formation of haze in cities with different energy consumption types also remain largely unknown.

In this study, we present the measurements of the NOCs and other chemical compositions in $PM_{2.5}$ collected from three cities (Haerbin, Beijing, and Hangzhou) with different energy consumption during winter. The specific objectives of this study were: (1) to investigate the differences in the abundance, composition, and major precursors of NOCs in different cities with different energy consumption, especially on polluted days; and (2) to elucidate the potential effects of ALW on the formation of oxidized NOCs (Ox-NOCs) and reduced NOCs (Re-NOCs) during winter (particularly on polluted days) in cities with different energy consumption. The research findings are expected to provide valuable implications for the mitigation of aerosol NOCs pollution in urban environments.

https://doi.org/10.5194/egusphere-2024-2602
Preprint. Discussion started: 7 October 2024

2. Materials and methods

2.1. Study site description and sample collection

The study sites are located in three urban areas, including Haerbin (HEB, i.e., Harbin, 126.64°E, 45.77°N), Beijing (BJ, 116.41°E, 40.04°N), and Hangzhou (HZ, 120.16°E, 30.30°N) (**Fig. S1**). The city of HEB, with a population density of 9.95 million, is situated in the northeastern region of China. It relies heavily on coal for centralized heating during winter. The rapid urbanization and increased coal consumption have significantly deteriorated air quality in HEB in recent years (Ma et al., 2020). In contrast, BJ has largely shifted towards the utilization of cleaner energy sources (e.g., natural gas) for centralized heating in recent years, particularly following the implementation of the "Beijing 2013–2017 Clean Air Action Plan" (Vu et al., 2019; Yuan et al., 2023). HZ, situated within the Yangtze River Delta, is exempt from the necessity of heating due to the relatively mild winter climate (average temperature of 6.6 ± 2.4 °C during the sampling period, **Table S1**). Clearly, the distinctive energy consumption patterns observed in these three cities during winter provide a valuable opportunity to examine the impact of various precursors and aqueous-phase processes on aerosol NOC formation.

Sample collection was carried out simultaneously in three cities from 16 December 2017 to 14 January 2018. $PM_{2.5}$ samples were collected every two or three days with a duration of 24 hours onto prebaked (450°C for ~10 hours) quartz fiber

https://doi.org/10.5194/egusphere-2024-2602
Preprint. Discussion started: 7 October 2024

filters (Pallflex, Pall Corporation, USA) using a high-volume air sampler (Series 2031, Laoying, China). One blank sample was collected at each sampling site. A total of 39 samples were collected, all of which were stored at −30°C. Meteorological data (e.g., temperature, relative humidity (RH) and wind speed) together with concentrations of various pollutants (e.g., SO_2 and NO_2) were obtained from nearby environmental stations. The sampling periods were classified as either "clean" or "haze" based on whether the daily average concentration of $PM_{2.5}$ was below or above 75 μg m^{-3} (Zhang and Cao, 2015; Xu et al., 2024).

2.2. Chemical analysis

The extraction and analysis methods for NOCs were consistent with those described in our recent publication (Ma et al., 2024). Briefly, a portion of each filter was extracted with methanol (LC-MS grade, CNW Technologies Ltd.) using sonication in an ice bath (~4°C). The extracts were filtered through a 0.22 μm polytetrafluoroethylene syringe filter and then concentrated to 300 μL under a gentle stream of nitrogen gas. The concentrated extracts underwent composition analysis via an ultra-performance liquid chromatography coupled with quadrupole time-of-flight mass spectrometry equipped with an electrospray ionization (ESI) source (UPLC-ESI-QToFMS, Waters Acquity Xevo G2-XS) (Wang et al., 2021c; Ma et al., 2024). This analysis was done in both ESI+ and ESI– modes. The organic compounds were

https://doi.org/10.5194/egusphere-2024-2602
Preprint. Discussion started: 7 October 2024

separated on a C_{18} column (2.1 × 100 mm, 1.7 μm particle size, Waters) with an 18-minute gradient elution. The mobile phases comprised ultrapure water with 0.1% formic acid (A) and methanol with 0.1% formic acid (B). Gradient elution was conducted according to the following protocol: 1% B was held for 1.5 minutes, followed by an increase to 54% B over a period of 6.5 minutes. Thereafter, the B was increased to 95% over a period of 3 minutes. After reaching 100% B in one minute, this state was maintained for 3 minutes. Finally, the concentration was returned to 1% B in 0.5 minutes and held for 2.5 minutes. Due to uncertainties in ionization efficiencies for different compounds (Ditto et al., 2022; Yang et al., 2023), an intercomparison (mainly compared among samples within this study) of compound relative abundance was conducted without accounting for differences in ionization efficiency in the present study. This consideration was consistent with previous studies (Xu et al., 2023; Jiang et al., 2022; Ma et al., 2024).

Another filter portion was ultrasonically extracted using Milli-Q water (~4°C ice bath) to analyze the concentrations of inorganic ions and organic acids. The inorganic ions (e.g., NO_3^-, SO_4^{2-}, Cl^-, Ca^{2+}, Mg^{2+}, Na^+, and NH_4^+) and organic acids (e.g., formic acid, acetic acid, oxalic acid, succinic acid, glutaric acid, and methanesulfonic acid) were quantified using an ion chromatograph system (Dionex Aquion, Thermo Scientific, USA) as described previously (Xu et al., 2022b; Yang et al., 2024b).

https://doi.org/10.5194/egusphere-2024-2602
Preprint. Discussion started: 7 October 2024

2.3. Compound categorization and precursor identification

The identified molecular formulas via UPLC-ESI-QToFMS were categorized into different compound classes based on their elemental compositions, which included CHO−, CHON−, CHONS−, and CHOS− in ESI− mode and CHO+, CHON+, and CHN+ in ESI+ mode (Ma et al., 2024). Here, we mainly focus on NOCs (i.e., CHN+, CHON+, and CHON− compounds) (Ma et al., 2024; Jiang et al., 2022; Wang et al., 2017). The carbon oxidation state (OS_C) and double bond equivalent (DBE) were calculated to indicate the oxidation level and unsaturation degree of the organics, respectively (**Sect. S1**) (Kroll et al., 2011; Ma et al., 2024). Additionally, the modified aromaticity index (AI_{mod}) and aromaticity equivalent (X_C) were used to evaluate aromaticity of organics (Koch and Dittmar, 2006), as detailed in **Sect. S1**.

The potential precursors of NOCs were identified based on the methodology outlined in previous studies (Nie et al., 2022; Guo et al., 2022; Jiang et al., 2023). The classification of CHON+ and CHON− compounds was refined into following categories, including aliphatics-, heterocyclics-, and aromatics-derived Re-NOCs and isoprene-, monoterpenes-, aliphatics-, and aromatics-derived Ox-NOCs. Moreover, CHN+ compounds were classified into aliphatic, monoaromatic, and polyaromatic CHN+ compound (Wang et al., 2021b; Yassine et al., 2014). A detailed description of the revised workflow for classifying NOCs according to potential precursors was provided in **Sect. S2** and **Fig. S2**.

https://doi.org/10.5194/egusphere-2024-2602
Preprint. Discussion started: 7 October 2024

187

188 **2.4. Classification of potential pathways for NOC formation**

189 To identify potential aqueous-phase processes for aerosol NOC formation, we
190 screened precursor-product pairs from the organic compounds that have been detected
191 (Su et al., 2021; Xu et al., 2023; Jiang et al., 2023). The reaction pathways of Re-
192 NOCs (mainly CHON+ compounds in this study) were refined into the following
193 categories, including condensation (cond_N), hydrolysis (hy_N), dehydration (de_N),
194 cond_hy_N (involving cond_N and hy_N), cond_de_N (involving cond_N and de_N),
195 hy_de_N (involving hy_N and de_N), cond_hy_de_N (involving cond_N, hy_N and
196 de_N) and unknown_N (unknown processes) formation pathways (**Fig. S3 and Table**
197 **S4**) (Sun et al., 2024; Abudumutailifu et al., 2024; Laskin et al., 2014; Liu et al.,
198 2023c). Another significant class of Re-NOCs is the CHN+ compounds. Their
199 potential formation mechanisms include cond_N, de_N, cond_de_N, and other
200 unidentified (unknown_N) pathways (**Fig. S4 and Table S4**) (Abudumutailifu et al.,
201 2024; Laskin et al., 2014; Liu et al., 2023c). In addition, the reaction pathways of Ox-
202 NOCs (mainly CHON− compounds in this study) were refined into the following
203 categories, including ox_N, hy_N, ox_hy_N (involving ox_N and hy_N), and other
204 unidentified (unknown_N) pathways (Jiang et al., 2023; Su et al., 2021) (**Fig. S5 and**
205 **Table S4**). A detailed overview of the methodologies employed to discern potential
206 NOC formation pathways was shown in **Sect. S3**, **Table S4,** and **Figs. S3–S5**.

https://doi.org/10.5194/egusphere-2024-2602
Preprint. Discussion started: 7 October 2024

It is important to acknowledge the potential limitations in the categorization methodology of NOC formation pathways described above. This is because the approach applied here and in previous studies (Jiang et al., 2023; Su et al., 2021) may classify NOCs from primary emissions as products of secondary aqueous-phase reactions. Accordingly, our results should be regarded as indicating a maximal potential (or an upper limit) for NOC generation from aqueous-phase reactions. In this study, NOCs produced from the reaction pathways identified by the abovementioned classification methodology can explain 76% of CHON+ compounds, 61% of CHN+ compounds, and 65% of CHON− compounds. Thus, the classification of potential pathways for NOC formation was representative, at least in this study.

2.5. More parameter calculations and data analysis

A thermodynamic model (ISORROPIA-II) was used to estimate the ALW concentration and pH value, as described in previous studies (Xu et al., 2020b; Xu et al., 2023; Xu et al., 2022c). Ambient hydroxyl radical (•OH) concentrations were predicted using empirical formulas proposed by Ehhalt and Rohrer (Ehhalt and Rohrer, 2000), which was reported in detail in our previous field observations (Liu et al., 2023a; Lin et al., 2023). The ventilation coefficient (VC) is an indicator of the potential for atmospheric dilution of pollutants, which was calculated by multiplying the wind speed by the planetary boundary layer height (PBLH) (Gani et al., 2019) .

https://doi.org/10.5194/egusphere-2024-2602
Preprint. Discussion started: 7 October 2024

Non-metric multidimensional scaling (NMDS) was employed to visualize the distributions of NOCs (CHON+, CHN+, and CHON– compounds) in two dimensions, based on Bray-Curtis distances (Chao et al., 2006). The stress values ranged from 0.03 to 0.11 (less than 0.2, **Table S5**) in our analysis, indicating that the differences among samples can be well represented in the two-dimensional pattern. To further assess the influence of anthropogenic emissions and aqueous-phase processes on the distribution of NOCs, the envfit function in the R package Vegan (Oksanen et al., 2007) was utilized. Furthermore, the Spearman rank correlation, a non-parametric measure with less sensitivity to outliers and independent of data distribution assumptions, was employed to examine the association patterns between NOCs and the parameters related to anthropogenic emissions and aqueous-phase processes (Kellerman et al., 2014).

3. Results and discussion

3.1. Overview of pollution and aerosol NOC characteristics in different cities

Figure 1a–c and **Table S1** show the variations in major gaseous pollutants, $PM_{2.5}$ and its major compositions, as well as meteorological parameters in three Chinese cities with different energy consumptions during winter. The average $PM_{2.5}$ concentration in HEB was 90.6 ± 62.4 μg m^{-3}, which was significantly higher than that observed in BJ (52.7 ± 51.4 μg m^{-3}) and HZ (69.1 ± 29.6 μg m^{-3}). Similarly, the

https://doi.org/10.5194/egusphere-2024-2602
Preprint. Discussion started: 7 October 2024

concentrations of SO_2 and nss-Cl^- were higher in HEB than in BJ and HZ. In addition, a lower NO_3^-/SO_4^{2-} mass ratio (**Table S1**) was found in HEB. SO_2 and nss-Cl^- have been suggested to be typical pollutants emitted from coal combustion during winter in cities (Zhao and Sun, 1986; Streets and Waldhoff, 2000). The low NO_3^-/SO_4^{2-} mass ratio can indicate a predominance of stationary sources (e.g., coal combustion) (Wang et al., 2006; Arimoto et al., 1996; Xiao and Liu, 2004). These results suggest that coal combustion during the winter heating season in HEB may significantly contributed to severe $PM_{2.5}$ pollution. This consideration can also be supported by the highest coal consumption in HEB in 2017–2018 (**Fig. 1d**). Due to the large-scale use of clean energy (i.e., natural gas) in BJ (**Fig. 1e**), the coal consumption in BJ was the lowest (**Fig. 1d**). This results in the lowest pollutant levels in BJ. From clean to polluted days, HEB and BJ showed larger increases in pollutant levels (e.g., $PM_{2.5}$, SO_2, and CO), followed by HZ. Thus, the release of pollutants caused by the use of fossil fuels for centralized heating in winter (only occurred in HEB and BJ) is undoubtedly one of the important factors contributing to the generation of haze in HEB and BJ.

https://doi.org/10.5194/egusphere-2024-2602
Preprint. Discussion started: 7 October 2024

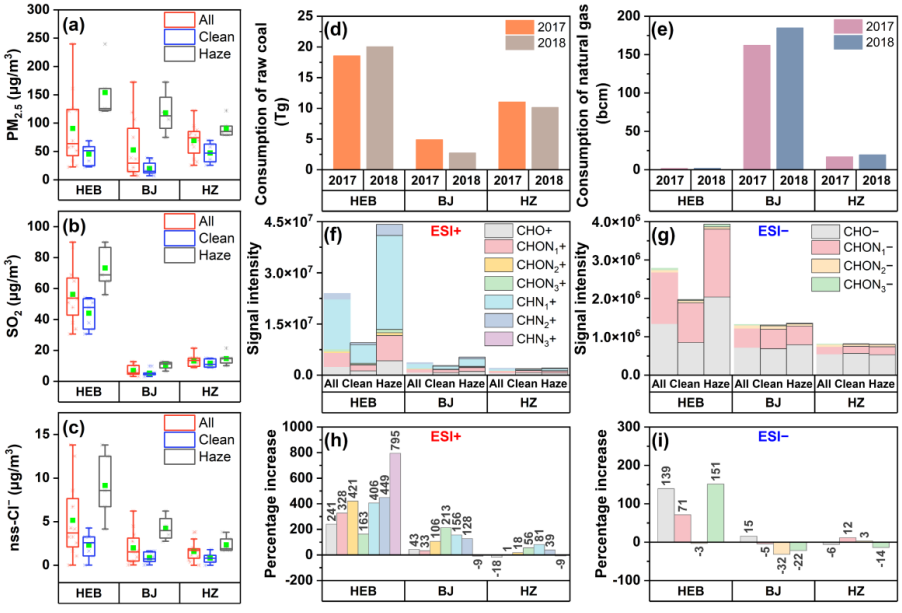

Figure 1. Box and whisker plots showing variations in the concentration of (**a**) $PM_{2.5}$, (**b**) SO_2, and (**c**) nss-Cl^-in all (gray), clean (blue), and haze (red) periods in different cities. Each box encompasses the 25th–75th percentiles. Whiskers are the 5th and 95th percentiles. The green squares and solid lines inside boxes indicate the mean and median value. The consumption of (**d**) raw coal and (**e**) natural gas in 2017 and 2018 in different cities was obtained from the local statistical yearbooks. Average distributions in the signal intensity of species detected in $PM_{2.5}$ collected during different winter periods in different cities in (**f**) ESI+ and (**g**) ESI− modes. Percentage variations in the signal intensity of each subgroup from clean to haze periods in different cities in (**h**) ESI+ and (**i**) ESI− modes.

https://doi.org/10.5194/egusphere-2024-2602
Preprint. Discussion started: 7 October 2024

Figure 1f and **g** show the average signal intensity distributions of organic compounds detected in $PM_{2.5}$ across sampling periods in different cities. The detailed mass spectra of organic compounds detected in ESI+ and ESI− were shown in **Fig. S6**. CHN_1+ (n = 437−448) compounds were the main CHN molecules measured in ESI+ mode in all cities (**Fig. 1f** and **Table S6**), the signal intensity of which accounted for over 77% of the total CHN_{1-3}+ signal intensity. Similarly, $CHON_1$+ compounds (n = 398−421) dominated in $CHON_{1-3}$+ molecules, with a higher signal intensity than $CHON_{2-3}$+ (**Fig. 1f** and **Table S6**). The high abundances of CHN_1+ and $CHON_1$+ compounds in NOCs were similar to previous reports about the NOC characteristics of urban aerosols (He et al., 2024; Abudumutailifu et al., 2024). The signal intensity fractions (40%−77%) of CHN+ compounds in total NOCs in these three cities were higher than those observed (8.20%−17.47%) during winter in Ürümqi where the same NOC analysis method was conducted (Ma et al., 2024). However, the signal intensity fractions of CHON+ compounds in total NOCs were lower in these three cities (23%−60%) than in Ürümqi (over 82.53%) (Ma et al., 2024). More frequent biomass burning and relatively dry climate in Ürümqi (northwest China) (Ma et al., 2024) may result in different sources and formation processes of NOCs compared to this study. The signal intensity of these NOCs detected in ESI+ mode varied across cities, with the highest CHN+ and CHON+ signal intensities in HEB, followed by BJ and HZ. Moreover, we found that the total signal intensities of CHN+ and CHON+ compounds

https://doi.org/10.5194/egusphere-2024-2602
Preprint. Discussion started: 7 October 2024

increased by 382% in HEB from clean to haze periods, followed by increase of 102% in BJ and increase of 31% in HZ (**Fig. 1h** and **Table S5**). This variation pattern of CHN+ and CHON+ compounds from clean to haze periods was similar to that of the pollutants mentioned previously (**Fig. 1a–c**). Given the high sensitivity of ESI+ mode to protonatable species, reduced species (e.g., amine- and amide-like compounds) were expected to predominate the NOCs (Han et al., 2023; Wang et al., 2018), the formation of which was highly related to precursor emission level, aerosol acidity, and ALW concentrations (Kuwata and Martin, 2012; Vione et al., 2005; Yang et al., 2024a; Xu et al., 2020b). Thus, these results suggest that there may be significant differences in the sources, precursor emission intensity, or main formation pathways of NOCs in different energy consuming cities.

The number of NOCs identified in ESI− (296–301 molecules excluding sulfur-containing compounds, **Table S7**) was found to be lower than that observed in ESI+ (1346–1361) (**Table S6**). This finding was similar to previous observations about the NOCs of urban organic aerosols in Beijing, Mainz, Changchun, Guangzhou, and Shanghai (Wang et al., 2021b; Wen et al., 2023; Wang et al., 2018). $CHON_1$− compounds were the main NOC molecules in ESI− mode in all cities (**Fig. 1g** and **Table S7**). The average signal intensity of CHON− compounds was highest in HEB, followed by BJ and HZ. Moreover, the outbreak of $CHON_{1-3}$ signal intensity during polluted periods was found in HEB, whereas insignificant increases occurred in BJ

https://doi.org/10.5194/egusphere-2024-2602
Preprint. Discussion started: 7 October 2024

and HZ (**Fig. 1i**). Deprotonated NOCs with oxidized nitrogen-functional groups, such as nitro (–NO_2) or nitrooxy (–ONO_2) groups, are more sensitive to the ESI− mode (Wang et al., 2017; Jiang et al., 2023; Yuan et al., 2023). Clearly, the formation of aerosol CHON− compounds was largely dependent on atmospheric oxidation capacity and gas- and aqueous-phase reactions (Ng et al., 2017; Shi et al., 2020; Shi et al., 2023). Thus, the differences in CHON− compound abundance in different polluted periods and cities together with the spatiotemporal changes in CHN+ and CHON+ abundances mentioned previously were likely attributed to variations in sources, mechanisms, or key influencing factors of NOC formation in these three cities, which will be further discussed in the following sections.

3.2. Potential precursors of aerosol NOCs in different cities

Figure 2 presents the average signal intensity percentage and signal intensity distributions of different NOCs from various precursors in different cities during winter. Aromatics-, heterocyclics-, and aliphatics-derived Re-NOCs together accounted for more than 74% (74%–79%) of the total signal intensity of CHON+ compounds in the three study cities (**Fig. 2a–c** and **Table S8**). Specifically, the proportion of the aromatics-derived CHON+ signal intensity in the total CHON+ signal intensity was much higher in HEB (73%) than in BJ (33%), with the lowest proportion observed in HZ (23%) (**Fig. 2a–c**). Furthermore, we observed that

https://doi.org/10.5194/egusphere-2024-2602
Preprint. Discussion started: 7 October 2024

aromatic CHN+ compounds (mono- and poly-aromatics) dominated the total CHN+ compounds in both number and abundance in all investigated cities (**Table S9** and **Fig. 2d–f**). The average signal intensity percentage and signal intensity of aromatic CHN+ compounds were also highest in HEB (**Fig. 2d–f** and **k**). The calculated AI_{mod} values for CHON+ and CHN+ compounds were higher in HEB than in BJ and HZ (**Table S10**), which further indicated a higher aromaticity of these NOCs in HEB. It has been suggested that coal combustion can release a large amount of aromatic compounds (Zhang et al., 2023a), which potentially increased NOC aromaticity (Yuan et al., 2023). Thus, the higher signal proportion of aromatics-derived Re-NOCs in HEB can be explained by the higher coal combustion emissions during winter. In contrast, the use of clean energy during the central heating season in BJ and the reduced emissions in HZ without central heating weakened the formation of aerosol aromatic NOCs.

CHON− compounds were also primarily dominated by aromatics-derived Ox-NOCs in all three cities, accounting for more than 73% (73%–90%) of the total signal intensity of CHON− compounds, on average (**Fig. 3g–i**). This finding was consistent with field observations conducted in other Chinese cities such as Shanghai, Changchun, Guangzhou, and Wangdu during winter (Wang et al., 2021b; Jiang et al., 2023). The abundance of aromatics-derived Ox-CHON− compounds and the AI_{mod} value of CHON− were highest in HEB and decreased sequentially in BJ and HZ (**Fig. 2h** and **Table S10**), further indicating our previous consideration that coal combustion

https://doi.org/10.5194/egusphere-2024-2602
Preprint. Discussion started: 7 October 2024

354 heating in HEB can lead to higher NOC pollution. It is worth noting that the
355 percentage of total signal intensity of Ox-NOCs with biogenic VOCs (BVOCs) as
356 precursors was less than 3% (**Fig. 2g–i** and **Table S8**). This can be partly supported by
357 the previous observations showing that anthropogenic VOCs (AVOCs) were the main
358 contributors to the formation of Ox-NOCs (e.g., organic nitrates) in urban areas in
359 China (Wang et al., 2021b; Jiang et al., 2023). The overall results suggest the
360 significant role of AVOCs in the formation of NOCs in all investigated cites,
361 particularly in HEB.

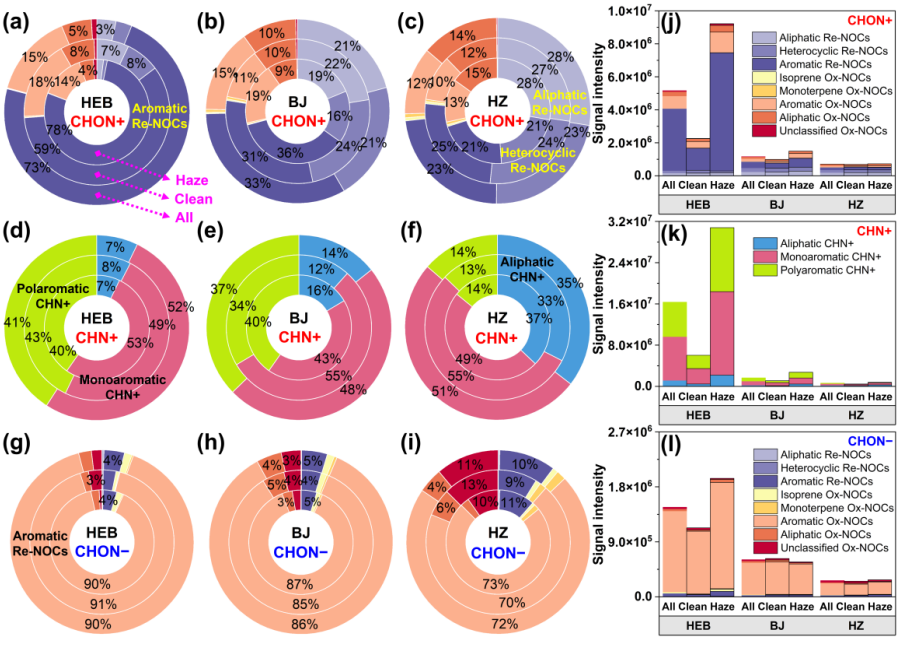

362

363 **Figure 2.** Average percentage distributions of signal intensities for (**a–c**) CHON+,
364 (**d–f**) CHN+, and (**g–i**) CHON− compounds from various sources in $PM_{2.5}$ collected
365 from different cities during winter. Average signal intensity distributions for (**j**)

https://doi.org/10.5194/egusphere-2024-2602
Preprint. Discussion started: 7 October 2024

CHON+, (**k**) CHN+, and (**l**) CHON− compounds from various sources in $PM_{2.5}$ collected from different cities during winter.

From clean to haze periods, the signal intensities of all aromatics-derived CHON compounds increased significantly in HEB (**Figs. 2a, j, g, l** and **S7**). In contrast, the signal intensities of aromatics-derived CHON compounds in BJ and HZ showed an insignificant increase during haze periods. In addition, the average values of O/C_w and OS_{Cw} for CHON+ and CHON− compounds were higher in HEB than in BJ (second highest) and HZ, and their increases from clean to haze periods were also greater in HEB (**Table S10**). This indicates that aerosol NOCs in HEB were more oxidized aromatics, particularly during haze. The average N/C_w ratios of CHON+ and CHON− compounds in HEB (0.13 and 0.15, respectively) (**Table S10**) were higher than those of CHON+ (0.079) and CHON− (0.07) compounds in aerosols directly emitted from coal combustion (Song et al., 2022; Song et al., 2018). The N/C_w ratios were also higher in HEB than in BJ and HZ and increased during hazy days (0.13 for CHON+ and 0.16 for CHON− in hazy days in HEB). It has been suggested that the N/C_w ratio of CHON− compounds tended to increase (from 0.109 to 0.119) after aging of fuel combustion-derived aerosols (Zhao et al., 2022a). Thus, these results, combined with previous analysis of potential precursors for NOCs, suggest that anthropogenic precursor emissions and their atmospheric transformation to form CHON compounds

https://doi.org/10.5194/egusphere-2024-2602
Preprint. Discussion started: 7 October 2024

were stronger in HEB than in BJ and HZ. Moreover, considering that the emission intensity of precursors during clean and hazy days may not significantly change, secondary processes may significantly promote the formation of NOCs in HEB during hazy days (the most significant increase in NOC abundance). However, this promoting effect during hazy days was insignificant in BJ and HZ (less increase in NOC abundance).

3.3. Main factors influencing aerosol NOC formation in different cities

The Spearman correlation analysis between various parameters and NOCs was conducted to investigate the key factors influencing NOC molecular distributions **(Fig. 3** and **Figs. S8−S12**). The peak intensity of most CHON+ compounds (mainly aromatics, as mentioned previously) showed a strong correlation ($P < 0.01$) with the concentrations of combustion source-related tracers (e.g., SO_2, nss-Cl^-, nss-K^+, CO, and NO_2) (Zhao and Sun, 1986; Streets and Waldhoff, 2000; Shen et al., 2009; Zhang et al., 2011; Mafusire et al., 2016; Liu et al., 2019; Zhang et al., 2021a; Wang et al., 2020) in HEB (**Figs. 3a** and **S8a–d**). Although there was a significant correlation ($P <$ 0.05) between most CHON+ compounds and those combustion source indicators in BJ, the strength of this correlation was weaker in BJ than in HEB (**Figs. 3e** and **S8f–i**). However, similar significant correlations between them were not observed in HZ (**Figs. 3i** and **S8k–n**). Thus, the greatest contribution of anthropogenic activities to the

https://doi.org/10.5194/egusphere-2024-2602
Preprint. Discussion started: 7 October 2024

406 formation of CHON+ compounds in winter was in HEB (central heating with coal),
407 followed by BJ (central heating with coal and natural gas) and HZ (without central
408 heating). Most of CHN+ and CHON− compounds showed a similar spatial response
409 pattern to those anthropogenic activities (**Figs. S9** and **S10**). These results are
410 consistent with the previous analysis of NOC precursors (**Fig. 2**), which concluded
411 that the intensity of anthropogenic pollutant emissions in different energy consuming
412 cities was an important factor affecting the formation of NOC and causing spatial
413 differences in NOC abundance.

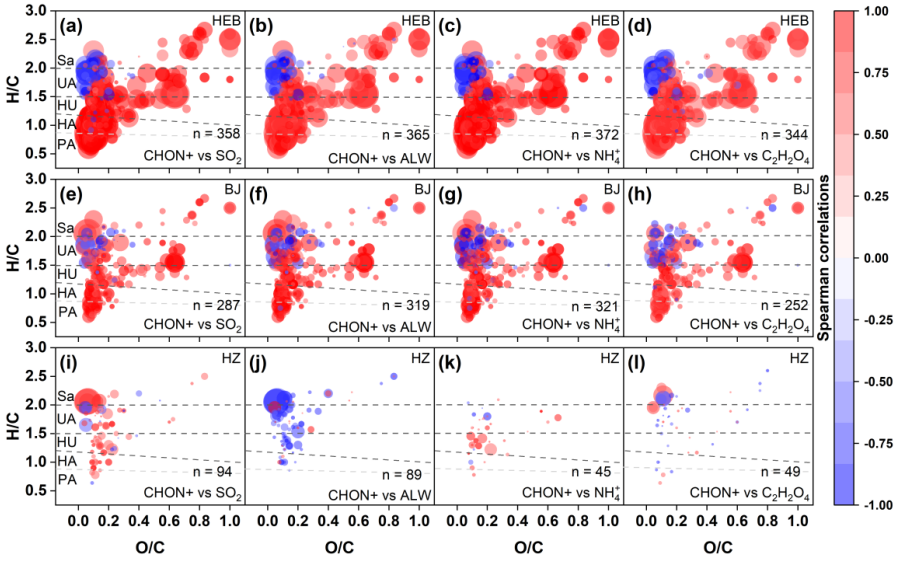

414

415 **Figure 3.** Spearman rank correlation coefficients (with $P < 0.01$ in HEB and $P < 0.05$
416 in BJ and HZ) of individual CHON+ molecules with selected parameters in (**a–d**)
417 HEB, (**e–h**) BJ and (**i–l**) HZ. The color scale indicates Spearman correlations between
418 the intensity of individual CHON+ molecules and each parameter. The symbol *n* in

https://doi.org/10.5194/egusphere-2024-2602
Preprint. Discussion started: 7 October 2024

the bottom right corner of each panel indicates the number of molecular formulas significantly correlated with the variables. The subgroups in the panels include polycyclic aromatic-like (PA), highly aromatic-like (HA), highly unsaturated-like (HU), unsaturated aliphatic-like (UA), and saturated-like (Sa) compounds.

Furthermore, we found that the peak intensities of most CHON+, CHN+, and CHON− compounds (mainly aromatics) were significantly correlated ($P < 0.01$) with the concentrations of ALW, NH_4^+, oxalic acid, and SO_4^{2-} (**Figs. 3b–d**, **S8e**, and **S11–S12**) in HEB. The correlations between these NOCs and parameters weakened in BJ and disappeared in HZ (**Figs. 3**, **S8**, and **S11–12**). It is generally accepted that SO_4^{2-}, NH_4^+, and NO_3^- in fine aerosols are primarily formed through secondary processes (Gao et al., 2021; Wang et al., 2021d). NH_4^+ can serve as a key reactant in the formation of aerosol NOCs (e.g., "carbonyl-to-imine" transformation) in the aqueous-phase (Laskin et al., 2014; Lee et al., 2013; Li et al., 2019b). Previous studies have identified oxalic acid ($C_2H_2O_4$) as a tracer for aqueous-phase SOA (Xu et al., 2022a; Carlton and Turpin, 2013). Additionally, numerous laboratory and field observational studies have shown that ALW can promote the formation of NOCs (Lv et al., 2022; Liu et al., 2023b; Jimenez et al., 2022; Jiang et al., 2023). Thus, these results indicate that aqueous-phase processes can significantly promote the formation of NOCs in HEB, however, as the precursor emission intensity gradually decreased in

https://doi.org/10.5194/egusphere-2024-2602
Preprint. Discussion started: 7 October 2024

BJ and HZ, this aqueous-phase promoting effect also decreased.

The NMDS analysis between various parameters and NOCs was conducted to further investigate the variations in key factors affecting the formation of NOCs from clean to haze days (**Fig. 4**). The formation of CHON+, CHN+, and CHON− compounds with higher AI_{mod} values (mainly aromatics, as mentioned previously) during haze days in HEB and BJ were closely associated with the factors indicating anthropogenic precursor emissions and aqueous-phase reaction processes. In contrast, the level of oxidants (i.e., O_3 and •OH) played a more important role during clean days in HEB and BJ, driving more highly saturated NOC formation during clean days (**Fig. 4**). A reasonable explanation for this is that the solar radiation and •OH levels on polluted days were lower than those on clean days (**Table S1**). The impacts of various factors on the formation of aerosol NOCs showed a weak discrimination between haze and clean days in HZ (**Fig. 4c, f** and **i**). Laboratory studies have shown that reactive components (e.g., •OH and H_2O_2) in the aqueous phase can continuously convert low-solubility organics to form aqueous phase SOA (Chen et al., 2008; Huang et al., 2011). Field observations also suggested that precursors (most of them are aromatic compounds) released from the combustion of fossil fuels significantly contributed to the aqueous SOA formation (> 50% total molecules) (Xu et al., 2022a) through the rapid aqueous-phase conversion of primary organic aerosol (POA) to SOA at high RH (Wang et al., 2021a). This implies that higher precursor abundance

https://doi.org/10.5194/egusphere-2024-2602
Preprint. Discussion started: 7 October 2024

can drive more aerosol NOC formation via aqueous-phase processes. As mentioned previously, the emission intensity of precursors decreased sequentially from HEB to BJ and then to HZ. Moreover, the ALW concentrations were much higher on polluted days than on clean days in three investigated cities. The rising ALW during the pollution period and the quiescent steady state of the atmosphere favored the formation of SOA from anthropogenic emission precursors (Guo et al., 2014; He et al., 2018). Thus, the above discussion can suggest that the spatial differences in precursor emission intensity (higher in HEB) and enhancement of aqueous-phase processes in polluted days were the main factors leading to the differences in the proportion (higher in HEB) of increase in NOC abundance from clean days to polluted days in three different energy consuming cities. In addition, the increased VC value (**Table S1**) in clean days (beneficial for the diffusion of pollutants) (Gani et al., 2019) was also an important factor limiting the abundance of NOCs (**Fig. 4**), resulting in a lower NOC abundance on clean days compared to polluted days (**Fig. 1**).

https://doi.org/10.5194/egusphere-2024-2602
Preprint. Discussion started: 7 October 2024

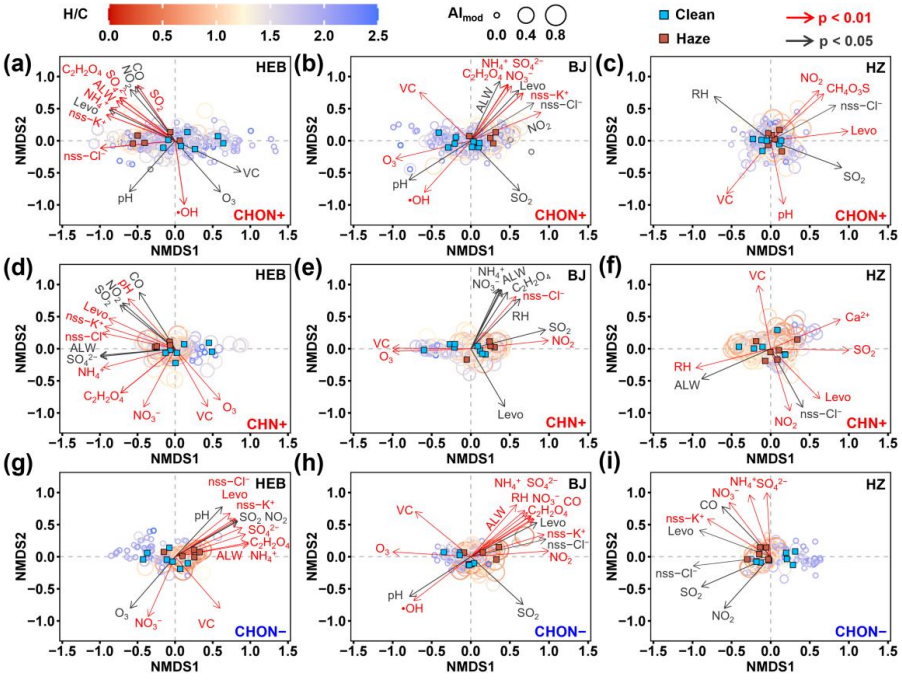

Figure 4. Nonmetric multidimensional scaling of (**a–c**) CHON+, (**d–f**) CHN+, and (**g–i**) CHON− compounds from organic aerosol in different cities. The color and size of the circle indicate the H/C ratio and AI_{mod} value of compounds, respectively. Significant relationships between the variables and ordination (999 permutations) are indicated by $p < 0.05$ (grey) and $p < 0.01$ (red). Insignificant correlations are not shown. The scores of the samples collected during clean and haze periods were shown as blue and brown squares, respectively.

As mentioned above, the aerosol NOCs of HZ were less affected by anthropogenic pollutants emitted from coal and natural gas combustion compared to

https://doi.org/10.5194/egusphere-2024-2602
Preprint. Discussion started: 7 October 2024

HEB and BJ with centralized heating. Interestingly, we found that the molecular distributions of most aromatic CHON+ compounds in HZ were not only influenced by some anthropogenic pollutants (e.g., SO_2 and NO_2), but also by methanesulfonic acid (CH_4O_3S) (**Fig. 4c**). Moreover, neither CHN+ nor CHON+ exhibited significant correlations with factors related to secondary processes in HZ (**Fig. 4c** and **f**). Methanesulfonic acid has been suggested to be a tracer for ocean aerosols (Ayers and Gras, 1991; Suess et al., 2019). These results suggest that aerosol CHON+ compounds in HZ may be influenced by long-distance transport air masses originating from the ocean. This consideration can be also supported by the fact that only HZ was affected by air masses originated from the ocean (**Fig. S13**). Thus, marine emissions may be an important contributor to aerosol NOCs in HZ, which was significantly different from the cases of HEB and BJ where aromatic pollutants from fossil fuel combustion and aqueous-phase processes control the composition and abundance of aerosol NOCs.

3.4. Potential formation mechanisms of aerosol NOCs in cities with different energy consumption

Figure 5 shows the average signal intensity percentage and signal intensity distributions of NOCs formed by different aqueous-phase processes (**Table S4** and **Figs. S3–S5**) in different cities during winter. The identification of specific reaction

https://doi.org/10.5194/egusphere-2024-2602
Preprint. Discussion started: 7 October 2024

pathways was detailed in **Figs. S3–S5** and **Sect. S3**. During the entire study period, the cond_N, cond_hy_N, and cond_de_N pathways together accounted for more than 68% (68%−74%) of the total signal intensity of CHON+ compounds in the three cities (**Fig. 5a–c** and **Table S11**). Specifically, the formation of CHON+ compounds was mainly dominated by the cond_N and cond_hy_N pathways in HEB, with less impact from the cond_de_N pathway (**Fig. 5a**). However, CHON+ compounds derived from the cond_de_N pathway showed a much higher proportion in BJ and HZ than in HEB (**Fig. 5b** and **c**). The cond_de_N pathway involves both condensation and dehydration processes (**Table S4 and Fig. S3**). It has been suggested that higher temperatures can facilitate the dehydration of amides into nitriles (Mekki-Berrada et al., 2013). The temperatures in BJ and HZ were higher than those in HEB (**Table S1**), which may partly explain the higher signal proportion of CHON+ compounds formed through the cond_hy_N pathway in BJ and HZ than in HEB. Furthermore, the higher signal proportions of CHN+ compounds formed through the de_N pathway in BJ (6%) and HZ (11%) than in HEB (2%) may also be associated with this temperature-induced dehydration mechanism (**Fig. 5d–f and Table S12**). For CHN+ compounds, the cond_de_N process dominated their formation (**Fig. 5d–f**). In general, the cond_N, cond_hy_N, and cond_de_N processes contributed most significantly to the formation of Re-NOCs in HEB, followed BJ and HZ.

https://doi.org/10.5194/egusphere-2024-2602
Preprint. Discussion started: 7 October 2024

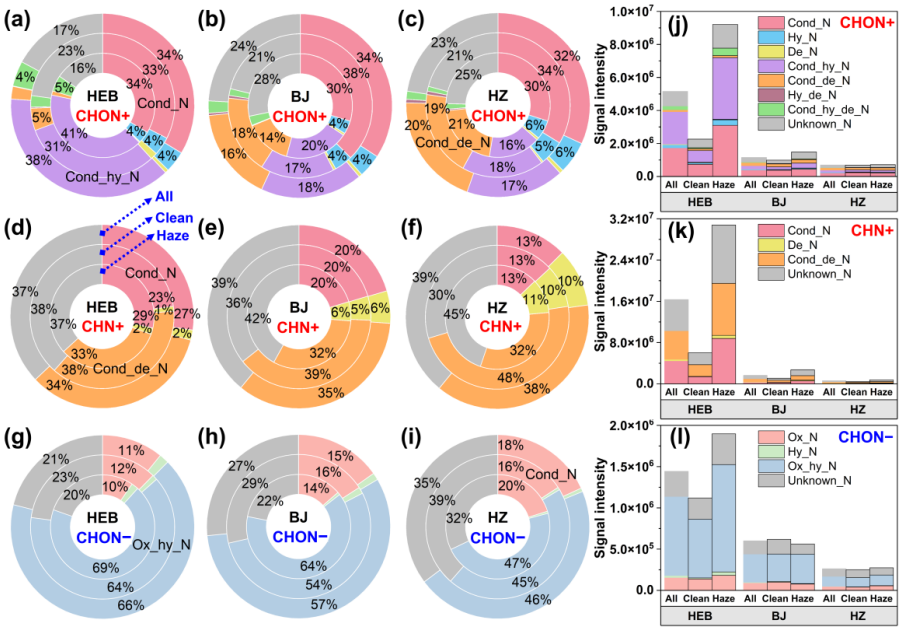

Figure 5. Average percentage distributions of signal intensities for aerosol (**a–c**) CHON+, (**d–f**) CHN+, and (**g–i**) CHON− compounds from various reaction pathways in different cities during winter. Average signal intensity distributions for aerosol (**j**) CHON+, (**k**) CHN+, and (**l**) CHON− compounds from various reaction pathways in different cities during winter.

A typical mechanism for Re-NOC formation is the aqueous-phase reactions between carbonyl compounds and NH_4^+ (or NH_3) (Abudumutailifu et al., 2024; Laskin et al., 2014; Li et al., 2019b; Liu et al., 2023b; Wang et al., 2024). If this mechanism is simplified as a second-order reaction (i.e., [Precursor] + [NH_3 and NH_4^+] ↔ [Re-NOCs]), the production of Re-NOCs is expected to be proportional to the

https://doi.org/10.5194/egusphere-2024-2602
Preprint. Discussion started: 7 October 2024

abundances of precursor and NH_4^+ (Yang et al., 2023; Lin et al., 2023). Indeed, the signal intensities of the Re-CHON+ and Re-CHN+ compounds were significantly positively correlated with the signal intensities of their CHO precursors (identified using the precursor-product pairs theory, **Figs. S3** and **S4**) and NH_4^+ concentration in HEB (**Fig. 6a, b, d and e**). This correlation gradually weakened from BJ to HZ (**Fig. 6a, b, d** and **e**). As previously discussed, differences in energy consumption patterns resulted in the highest levels of anthropogenic aromatic compound emissions in HEB during the winter, followed by BJ, with the lowest levels in HZ (**Figs. 2** and **S14**). Thus, the signal intensities of CHON+ and CHN+ compounds from cond_N, cond_de_N, and cond_hy_N processes were higher in HEB than in BJ and lowest in HZ (**Fig. 5j** and **k**).

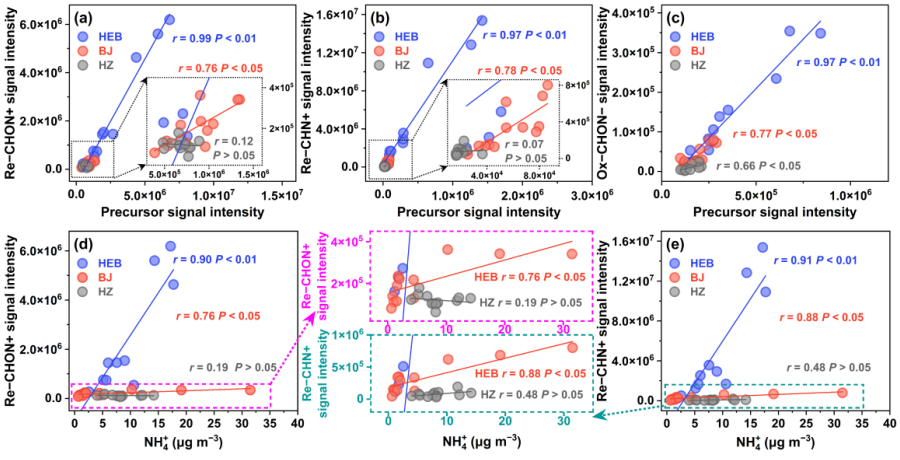

Figure 6. Signal intensity of (**a**) Re-CHON+, (**b**) Re-CHN+, and (**c**) Ox-CHON− compounds as functions of signal intensity of precursors (CHO compounds). Signal intensity of (**d**) Re-CHON+ and (**e**) Re-CHN+ compounds as functions of the

https://doi.org/10.5194/egusphere-2024-2602
Preprint. Discussion started: 7 October 2024

concentrations of NH_4^+.

Additionally, we noticed that the contribution of these aqueous-phase processes to the formation of CHON+ and CHN+ compounds increased significantly from clean to hazy days in HEB and BJ (**Fig. 5**). The increased ALW concentrations (**Table S1**) and atmospheric stability during haze periods likely provided favorable conditions for the precursors to undergo these aqueous-phase reactions, resulting in the formation of NOCs. Clearly, high pollutant emission levels in HEB provided a greater potential to convert precursors into more NOCs via the cond_N, cond_hy_N, and cond_de_N processes during haze periods. Thus, the hazy days in the HEB showed the largest increase in CHON+ and CHN+ compounds from the cond_N, cond_hy_N, and cond_de_N processes (**Fig. 5j** and **k**). In contrast, the lower precursor emissions in HZ without centralized heating policy were not sufficient to support the production of large amounts of NOCs in the aqueous phase. These results also indicate that emission reduction is the key to controlling aerosol NOC pollution.

CHON− compounds derived from the ox_hy_N and ox_N processes together accounted for more than 64% (64%−71%) of the total signal intensity of CHON− compounds in the three cities (**Fig. 5g–i, l** and **Table S13**). The signal intensity proportions of CHON− compounds formed by the ox_hy_N process in these three cities (ranging from 47% in HZ to 69% in HEB) were higher than that in Wangdu (<

https://doi.org/10.5194/egusphere-2024-2602
Preprint. Discussion started: 7 October 2024

20%) (Jiang et al., 2023). The observation study in Wangdu examined aerosol organic components only in ESI− mode (Jiang et al., 2023), which may underestimate the importance of the CHO+ compounds that could serve as precursors of Ox-NOCs. In general, CHON− compounds formed through the ox_hy_N and ox_N processes showed the highest abundance in HEB, followed by BJ and HZ (**Fig. 5j–i**). According to a simplified reaction mechanism for the formation of Ox-NOCs via aqueous-phase processes (i.e., [Precursor] + [Oxidants] ↔ [Ox-NOCs]) (Shi et al., 2023; Kroflič et al., 2015; Vione et al., 2005), we can infer that Ox-NOCs production is proportional to precursor levels when oxidants (e.g., NO_2 radical or NO_2^+) are in a steady state in the atmosphere. Indeed, the signal intensities of the Ox-CHON− compounds were significantly positively correlated with the signal intensities of their CHO precursors identified using the precursor-product pairs theory in HEB (**Fig. 6c**). Moreover, this correlation gradually weakened from BJ to HZ (**Fig. 6c**). Thus, the spatial differences in the contribution of the ox_hy_N and ox_N processes to Ox-NOC production across the three cities can also be explained by differences in precursor emission intensity, as indicated by above mentioned Re-NOC formation.

4. Conclusion

The abundance, composition, potential precursors, and potential formation mechanisms of NOCs in $PM_{2.5}$ in three Chinese cities with different energy

https://doi.org/10.5194/egusphere-2024-2602
Preprint. Discussion started: 7 October 2024

consumption types during the winter were systematically investigated. On average, the total signal intensity of NOCs (i.e., CHN+, CHON+, and CHON− compounds) was highest in HEB, followed by BJ. The lowest total NOC signal intensity was found in HZ. According to the identification of potential precursors of NOCs, we found that anthropogenic aromatic compounds were the main precursors of NOCs during winter in HEB where mainly relies on coal for winter heating, with less impact from BVOCs. Anthropogenic aromatic precursors were also identified to be important contributors to NOC formation in BJ which uses natural gas and coal for winter heating, although the contribution ratio was lower in BJ than in HEB. In contrast, the lowest aromatic precursor levels occurred in HZ without winter heating policy. Furthermore, the NMDS analysis supported that the impact of anthropogenic fossil fuel combustion on NOC pollution gradually decreased from HEB to BJ and then to HZ.

The formation of CHON+ compounds was mainly associated with the cond_N, cond_hy_N, and cond_de_N processes. The cond_N and cond_de_N processes dominated the formation of CHN+ compounds. The production of CHON+ and CHN+ compounds from the cond_N, cond_hy_N, and cond_de_N processes was highest in HEB, followed by BJ and HZ. The ox_hy_N and ox_N processes contributed significantly to CHON− compound formation, from which the highest CHON− production occurred in HEB and the lowest in HZ. The spatial differences in the contribution of different aqueous-phase processes to NOC production in the three

https://doi.org/10.5194/egusphere-2024-2602
Preprint. Discussion started: 7 October 2024

610 different cities can be attributed to differences in precursor emission intensity. In
611 particular, the contribution of these aqueous-phase processes to the formation of
612 CHON+ and CHN+ compounds showed the most significant increase from clean to
613 hazy days in HEB, followed by BJ. We concluded that high pollutant emission levels
614 can provide a greater potential to convert precursors to produce more NOCs via
615 aqueous-phase processes during haze periods. The above findings are summarized in
616 a diagram (**Fig. 7**).

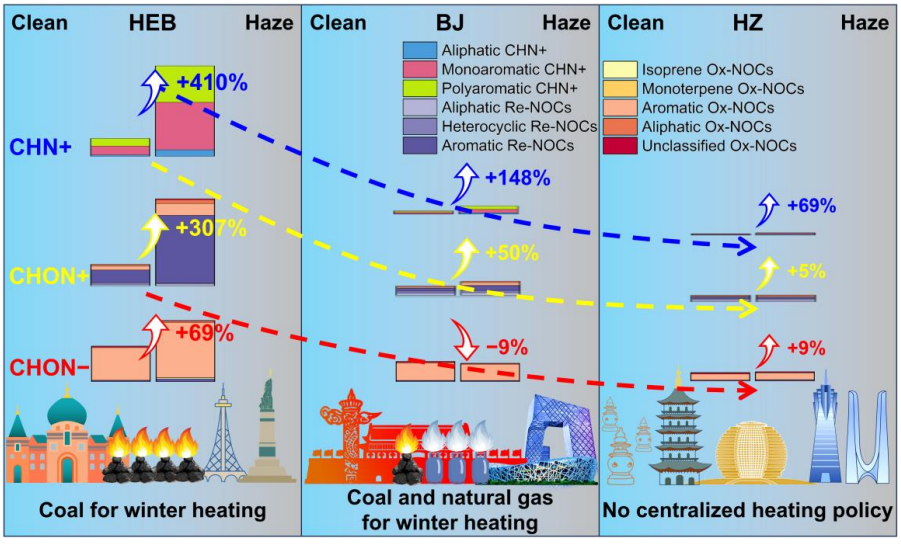

617

618 **Figure 7**. Conceptual illustration showing the characteristics of different NOCs from
619 the clean days to the haze days in different cities.

620 In general, the aerosol NOCs pollution during winter is closely linked to both the
621 intensity of precursor emissions and the efficiency of aqueous-phase processes in
622 converting these emissions into NOCs. The overall results highlight the importance of

https://doi.org/10.5194/egusphere-2024-2602
Preprint. Discussion started: 7 October 2024

emission reduction strategies in controlling aerosol NOCs pollution during winter. Targeted reduction of precursor emissions, especially from coal combustion, could significantly mitigate NOCs levels, thereby improving air quality and public health in urban areas. Future research should focus on further elucidating the specific pathways of aqueous-phase NOC formation and developing available models to predict NOC dynamics under varying environmental conditions. Additionally, research into the long-term effects of transitioning to cleaner energy sources on the reduction of NOC pollution will be essential for guiding effective air quality management strategies.

Data availability. The data presented in this work are available upon request from the corresponding authors.

Competing interests. The authors declare no conflicts of interest relevant to this study.

Supplement. Details of parameter calculation, classification method for identifying precursors of NOCs, classification of possible aqueous-phase processes NOCs based on precursor-product pairs, thirteen tables (Tables S1−S13), and fourteen extensive figures (Figures S1−S14) are provided in the Supplement.

https://doi.org/10.5194/egusphere-2024-2602
Preprint. Discussion started: 7 October 2024

Author contributions. YX designed the study. YJM, TY, LG, HX, and HWX performed field measurements and sample collection; YJM performed chemical analysis; YX and YJM performed data analysis; YJM and YX wrote the original manuscript; and YX, YJM, and HYX reviewed and edited the manuscript.

Financial support. This study was kindly supported by the National Natural Science Foundation of China through grant 42303081 (Y. Xu) and Shanghai "Science and Technology Innovation Action Plan" Shanghai Sailing Program through grant 22YF1418700 (Y. Xu).

References

Abudumutailifu, M., Shang, X., Wang, L., Zhang, M., Kang, H., Chen, Y., Li, L., Ju, R., Li, B., Ouyang, H., Tang, X., Li, C., Wang, L., Wang, X., George, C., Rudich, Y., Zhang, R., and Chen, J.: Unveiling the Molecular Characteristics, Origins, and Formation Mechanism of Reduced Nitrogen Organic Compounds in the Urban Atmosphere of Shanghai Using a Versatile Aerosol Concentration Enrichment System, Environ. Sci. Technol., 10.1021/acs.est.3c04071, 2024.

Arimoto, R., Duce, R. A., Savoie, D. L., Prospero, J. M., Talbot, R., Cullen, J. D., Tomza, U., Lewis, N. F., and Ray, B. J.: Relationships among aerosol constituents from Asia and the North Pacific during PEM-West A, J. Geophys. Res.-Atmos., 101,

https://doi.org/10.5194/egusphere-2024-2602
Preprint. Discussion started: 7 October 2024

2011-2023, https://doi.org/10.1029/95JD01071, 1996.

Ayers, G. P. and Gras, J. L.: Seasonal relationship between cloud condensation nuclei and aerosol methanesulphonate in marine air, Nature, 353, 834-835, 10.1038/353834a0, 1991.

Bond, T. C., Wehner, B., Plewka, A., Wiedensohler, A., Heintzenberg, J., and Charlson, R. J.: Climate-relevant properties of primary particulate emissions from oil and natural gas combustion, Atmos. Environ., 40, 3574-3587, https://doi.org/10.1016/j.atmosenv.2005.12.030, 2006.

Cape, J. N., Cornell, S. E., Jickells, T. D., and Nemitz, E.: Organic nitrogen in the atmosphere — Where does it come from? A review of sources and methods, Atmos. Res., 102, 30-48, https://doi.org/10.1016/j.atmosres.2011.07.009, 2011.

Carlton, A. G. and Turpin, B. J.: Particle partitioning potential of organic compounds is highest in the Eastern US and driven by anthropogenic water, Atmos. Chem. Phys., 13, 10203-10214, 10.5194/acp-13-10203-2013, 2013.

Chao, A., Chazdon, R. L., Colwell, R. K., and Shen, T.-J.: Abundance-Based Similarity Indices and Their Estimation When There Are Unseen Species in Samples, Biometrics, 62, 361-371, https://doi.org/10.1111/j.1541-0420.2005.00489.x, 2006.

Chen, Z. M., Wang, H. L., Zhu, L. H., Wang, C. X., Jie, C. Y., and Hua, W.: Aqueous-phase ozonolysis of methacrolein and methyl vinyl ketone: a potentially important source of atmospheric aqueous oxidants, Atmos. Chem. Phys., 8, 2255-

https://doi.org/10.5194/egusphere-2024-2602
Preprint. Discussion started: 7 October 2024

683 2265, 10.5194/acp-8-2255-2008, 2008.

684 Ditto, J. C., Machesky, J., and Gentner, D. R.: Analysis of reduced and oxidized
685 nitrogen-containing organic compounds at a coastal site in summer and winter, Atmos.
686 Chem. Phys., 22, 3045-3065, https://doi.org/10.5194/acp-22-3045-2022, 2022.

687 Ehhalt, D. H. and Rohrer, F.: Dependence of the OH concentration on solar UV, J.
688 Geophys. Res.-Atmos., 105, 3565-3571, https://doi.org/10.1029/1999JD901070, 2000.

689 Gani, S., Bhandari, S., Seraj, S., Wang, D. S., Patel, K., Soni, P., Arub, Z., Habib,
690 G., Hildebrandt Ruiz, L., and Apte, J. S.: Submicron aerosol composition in the
691 world's most polluted megacity: the Delhi Aerosol Supersite study, Atmos. Chem.
692 Phys., 19, 6843-6859, 10.5194/acp-19-6843-2019, 2019.

693 Gao, J., Li, Y., Li, J., Shi, G., Liu, Z., Han, B., Tian, X., Wang, Y., Feng, Y., and
694 Russell, A. G.: Impact of Formation Pathways on Secondary Inorganic Aerosol
695 During Haze Pollution in Beijing: Quantitative Evidence From High-Resolution
696 Observation and Modeling, Geophys. Res. Lett., 48, e2021GL095623,
697 https://doi.org/10.1029/2021GL095623, 2021.

698 Guo, S., Hu, M., Zamora, M. L., Peng, J., Shang, D., Zheng, J., Du, Z., Wu, Z.,
699 Shao, M., Zeng, L., Molina, M. J., and Zhang, R.: Elucidating severe urban haze
700 formation in China, P. Natl. Acad. Sci. USA, 111, 17373-17378,
701 doi:10.1073/pnas.1419604111, 2014.

702 Guo, Y., Yan, C., Liu, Y., Qiao, X., Zheng, F., Zhang, Y., Zhou, Y., Li, C., Fan, X.,

https://doi.org/10.5194/egusphere-2024-2602
Preprint. Discussion started: 7 October 2024

703 Lin, Z., Feng, Z., Zhang, Y., Zheng, P., Tian, L., Nie, W., Wang, Z., Huang, D.,
704 Daellenbach, K. R., Yao, L., Dada, L., Bianchi, F., Jiang, J., Liu, Y., Kerminen, V. M.,
705 and Kulmala, M.: Seasonal variation in oxygenated organic molecules in urban
706 Beijing and their contribution to secondary organic aerosol, Atmos. Chem. Phys., 22,
707 10077-10097, 10.5194/acp-22-10077-2022, 2022.

708 Hallquist, M., Wenger, J. C., Baltensperger, U., Rudich, Y., Simpson, D., Claeys,
709 M., Dommen, J., Donahue, N. M., George, C., Goldstein, A. H., Hamilton, J. F.,
710 Herrmann, H., Hoffmann, T., Iinuma, Y., Jang, M., Jenkin, M. E., Jimenez, J. L.,
711 Kiendler-Scharr, A., Maenhaut, W., McFiggans, G., Mentel, T. F., Monod, A., Prévôt,
712 A. S. H., Seinfeld, J. H., Surratt, J. D., Szmigielski, R., and Wildt, J.: The formation,
713 properties and impact of secondary organic aerosol: current and emerging issues,
714 Atmos. Chem. Phys., 9, 5155-5236, 10.5194/acp-9-5155-2009, 2009.

715 Han, Y., Zhang, X., Li, L., Lin, Y., Zhu, C., Zhang, N., Wang, Q., and Cao, J.:
716 Enhanced Production of Organosulfur Species during a Severe Winter Haze Episode
717 in the Guanzhong Basin of Northwest China, Environ. Sci. Technol.,
718 https://doi.org/10.1021/acs.est.3c02914, 2023.

719 He, C., Che, H., Bao, Z., Liu, Y., Li, Q., Hu, M., Zhou, J., Zhang, S., Yao, X., Shi,
720 Q., Chen, C., Han, Y., Meng, L., Long, X., Yang, F., and Chen, Y.: Evolution of
721 nucleophilic high molecular-weight organic compounds in ambient aerosols: a case
722 study, Atmos. Chem. Phys., 24, 1627-1639, 10.5194/acp-24-1627-2024, 2024.

https://doi.org/10.5194/egusphere-2024-2602
Preprint. Discussion started: 7 October 2024

He, Q.-F., Ding, X., Fu, X.-X., Zhang, Y.-Q., Wang, J.-Q., Liu, Y.-X., Tang, M.-J., Wang, X.-M., and Rudich, Y.: Secondary Organic Aerosol Formation From Isoprene Epoxides in the Pearl River Delta, South China: IEPOX- and HMML-Derived Tracers, J. Geophys. Res.-Atmos., 123, 6999-7012, https://doi.org/10.1029/2017JD028242, 2018.

Hodas, N., Sullivan, A. P., Skog, K., Keutsch, F. N., Collett, J. L., Jr., Decesari, S., Facchini, M. C., Carlton, A. G., Laaksonen, A., and Turpin, B. J.: Aerosol Liquid Water Driven by Anthropogenic Nitrate: Implications for Lifetimes of Water-Soluble Organic Gases and Potential for Secondary Organic Aerosol Formation, Environ. Sci. Technol., 48, 11127-11136, 10.1021/es5025096, 2014.

Huang, D., Zhang, X., Chen, Z. M., Zhao, Y., and Shen, X. L.: The kinetics and mechanism of an aqueous phase isoprene reaction with hydroxyl radical, Atmos. Chem. Phys., 11, 7399-7415, 10.5194/acp-11-7399-2011, 2011.

Huang, S., Shen, Z., Yang, X., Bai, G., Zhang, L., Zeng, Y., Sun, J., Xu, H., Ho, S. S. H., Zhang, Y., and Cao, J.: Nitroaromatic compounds in six major Chinese cities: Influence of different formation mechanisms on light absorption properties, Sci. Total Environ., 930, 172672, https://doi.org/10.1016/j.scitotenv.2024.172672, 2024.

Jiang, H., Li, J., Tang, J., Zhao, S., Chen, Y., Tian, C., Zhang, X., Jiang, B., Liao, Y., and Zhang, G.: Factors Influencing the Molecular Compositions and Distributions of Atmospheric Nitrogen-Containing Compounds, J. Geophys. Res.-Atmos., 127,

https://doi.org/10.5194/egusphere-2024-2602
Preprint. Discussion started: 7 October 2024

743 e2021JD036284, https://doi.org/10.1029/2021JD036284, 2022.

744 Jiang, H., Cai, J., Feng, X., Chen, Y., Wang, L., Jiang, B., Liao, Y., Li, J., Zhang,
745 G., Mu, Y., and Chen, J.: Aqueous-Phase Reactions of Anthropogenic Emissions Lead
746 to the High Chemodiversity of Atmospheric Nitrogen-Containing Compounds during
747 the Haze Event, Environ. Sci. Technol., 57, 16500-16511, 10.1021/acs.est.3c06648,
748 2023.

749 Jimenez, N. G., Sharp, K. D., Gramyk, T., Ugland, D. Z., Tran, M.-K., Rojas, A.,
750 Rafla, M. A., Stewart, D., Galloway, M. M., Lin, P., Laskin, A., Cazaunau, M., Pangui,
751 E., Doussin, J.-F., and De Haan, D. O.: Radical-Initiated Brown Carbon Formation in
752 Sunlit Carbonyl–Amine–Ammonium Sulfate Mixtures and Aqueous Aerosol Particles,
753 ACS Earth Space Chem., 6, 228-238, 10.1021/acsearthspacechem.1c00395, 2022.

754 Kellerman, A. M., Dittmar, T., Kothawala, D. N., and Tranvik, L. J.:
755 Chemodiversity of dissolved organic matter in lakes driven by climate and hydrology,
756 Nature Communications, 5, 3804, 10.1038/ncomms4804, 2014.

757 Koch, B. P. and Dittmar, T.: From mass to structure: an aromaticity index for
758 high-resolution mass data of natural organic matter, Rapid Commun. Mass Spectrom.,
759 20, 926-932, https://doi.org/10.1002/rcm.2386, 2006.

760 Kroflič, A., Grilc, M., and Grgić, I.: Does toxicity of aromatic pollutants increase
761 under remote atmospheric conditions?, Scientific Reports, 5, 8859,
762 10.1038/srep08859, 2015.

https://doi.org/10.5194/egusphere-2024-2602
Preprint. Discussion started: 7 October 2024

763 Kroll, J. H., Donahue, N. M., Jimenez, J. L., Kessler, S. H., Canagaratna, M. R.,
764 Wilson, K. R., Altieri, K. E., Mazzoleni, L. R., Wozniak, A. S., Bluhm, H., Mysak, E.
765 R., Smith, J. D., Kolb, C. E., and Worsnop, D. R.: Carbon oxidation state as a metric
766 for describing the chemistry of atmospheric organic aerosol, Nat. Chem., 3, 133-139,
767 https://doi.org/10.1038/nchem.948, 2011.
768 Křůmal, K., Mikuška, P., Horák, J., Hopan, F., and Krpec, K.: Comparison of
769 emissions of gaseous and particulate pollutants from the combustion of biomass and
770 coal in modern and old-type boilers used for residential heating in the Czech Republic,
771 Central Europe, Chemosphere, 229, 51-59,
772 https://doi.org/10.1016/j.chemosphere.2019.04.137, 2019.
773 Kuwata, M. and Martin, S. T.: Phase of atmospheric secondary organic material
774 affects its reactivity, P. Natl. Acad. Sci. USA, 109, 17354-17359,
775 doi:10.1073/pnas.1209071109, 2012.
776 Laskin, J., Laskin, A., Nizkorodov, S. A., Roach, P., Eckert, P., Gilles, M. K.,
777 Wang, B., Lee, H. J., and Hu, Q.: Molecular Selectivity of Brown Carbon
778 Chromophores, Environ. Sci. Technol., 48, 12047-12055,
779 https://doi.org/10.1021/es503432r, 2014.
780 Lee, A. K. Y., Zhao, R., Li, R., Liggio, J., Li, S.-M., and Abbatt, J. P. D.:
781 Formation of Light Absorbing Organo-Nitrogen Species from Evaporation of
782 Droplets Containing Glyoxal and Ammonium Sulfate, Environ. Sci. Technol., 47,

https://doi.org/10.5194/egusphere-2024-2602
Preprint. Discussion started: 7 October 2024

12819-12826, 10.1021/es402687w, 2013.

Li, X., Song, S., Zhou, W., Hao, J., Worsnop, D. R., and Jiang, J.: Interactions between aerosol organic components and liquid water content during haze episodes in Beijing, Atmos. Chem. Phys., 19, 12163-12174, 10.5194/acp-19-12163-2019, 2019a.

Li, Y., Fu, T.-M., Yu, J. Z., Yu, X., Chen, Q., Miao, R., Zhou, Y., Zhang, A., Ye, J., Yang, X., Tao, S., Liu, H., and Yao, W.: Dissecting the contributions of organic nitrogen aerosols to global atmospheric nitrogen deposition and implications for ecosystems, National Science Review, 10, 10.1093/nsr/nwad244, 2023.

Li, Z., Nizkorodov, S. A., Chen, H., Lu, X., Yang, X., and Chen, J.: Nitrogen-containing secondary organic aerosol formation by acrolein reaction with ammonia/ammonium, Atmos. Chem. Phys., 19, 1343-1356, 10.5194/acp-19-1343-2019, 2019b.

Lin, X., Xu, Y., Zhu, R.-G., Xiao, H.-W., and Xiao, H.-Y.: Proteinaceous Matter in $PM_{2.5}$ in Suburban Guiyang, Southwestern China: Decreased Importance in Long-Range Transport and Atmospheric Degradation, J. Geophys. Res.-Atmos., 128, e2023JD038516, https://doi.org/10.1029/2023JD038516, 2023.

Liu, T., Xu, Y., Sun, Q.-B., Xiao, H.-W., Zhu, R.-G., Li, C.-X., Li, Z.-Y., Zhang, K.-Q., Sun, C.-X., and Xiao, H.-Y.: Characteristics, Origins, and Atmospheric Processes of Amines in Fine Aerosol Particles in Winter in China, J. Geophys. Res.-Atmos., 128, e2023JD038974, https://doi.org/10.1029/2023JD038974, 2023a.

https://doi.org/10.5194/egusphere-2024-2602
Preprint. Discussion started: 7 October 2024

Liu, X.-Y., He, K.-B., Zhang, Q., Lu, Z.-F., Wang, S.-W., Zhang, Y.-X., and Streets, D. G.: Analysis of the origins of black carbon and carbon monoxide transported to Beijing, Tianjin, and Hebei in China, Sci. Total Environ., 653, 1364-1376, https://doi.org/10.1016/j.scitotenv.2018.09.274, 2019.

Liu, X., Wang, H., Wang, F., Lv, S., Wu, C., Zhao, Y., Zhang, S., Liu, S., Xu, X., Lei, Y., and Wang, G.: Secondary Formation of Atmospheric Brown Carbon in China Haze: Implication for an Enhancing Role of Ammonia, Environ. Sci. Technol., 57, 11163-11172, 10.1021/acs.est.3c03948, 2023b.

Liu, Z., Zhu, B., Zhu, C., Ruan, T., Li, J., Chen, H., Li, Q., Wang, X., Wang, L., Mu, Y., Collett, J., George, C., Wang, Y., Wang, X., Su, J., Yu, S., Mellouki, A., Chen, J., and Jiang, G.: Abundant nitrogenous secondary organic aerosol formation accelerated by cloud processing, iScience, 26, 108317, https://doi.org/10.1016/j.isci.2023.108317, 2023c.

Lv, S., Wang, F., Wu, C., Chen, Y., Liu, S., Zhang, S., Li, D., Du, W., Zhang, F., Wang, H., Huang, C., Fu, Q., Duan, Y., and Wang, G.: Gas-to-Aerosol Phase Partitioning of Atmospheric Water-Soluble Organic Compounds at a Rural Site in China: An Enhancing Effect of NH3 on SOA Formation, Environ. Sci. Technol., 56, 3915-3924, 10.1021/acs.est.1c06855, 2022.

Ma, L., Li, B., Liu, Y., Sun, X., Fu, D., Sun, S., Thapa, S., Geng, J., Qi, H., Zhang, A., and Tian, C.: Characterization, sources and risk assessment of PM2.5-

https://doi.org/10.5194/egusphere-2024-2602
Preprint. Discussion started: 7 October 2024

bound polycyclic aromatic hydrocarbons (PAHs) and nitrated PAHs (NPAHs) in Harbin, a cold city in Northern China, Journal of Cleaner Production, 264, 121673, https://doi.org/10.1016/j.jclepro.2020.121673, 2020.

Ma, Y. J., Xu, Y., Yang, T., Xiao, H. W., and Xiao, H. Y.: Measurement report: Characteristics of nitrogen-containing organics in $PM_{2.5}$ in Ürümqi, northwestern China – differential impacts of combustion of fresh and aged biomass materials, Atmos. Chem. Phys., 24, 4331-4346, 10.5194/acp-24-4331-2024, 2024.

Mafusire, G., Annegarn, H. J., Vakkari, V., Beukes, J. P., Josipovic, M., van Zyl, P. G., and Laakso, L.: Submicrometer aerosols and excess CO as tracers for biomass burning air mass transport over southern Africa, J. Geophys. Res.-Atmos., 121, 10,262-210,282, https://doi.org/10.1002/2015JD023965, 2016.

Mekki-Berrada, A., Bennici, S., Gillet, J.-P., Couturier, J.-L., Dubois, J.-L., and Auroux, A.: Ammoniation–Dehydration of Fatty Acids into Nitriles: Heterogeneous or Homogeneous Catalysis?, ChemSusChem, 6, 1478-1489, https://doi.org/10.1002/cssc.201300210, 2013.

Montoya-Aguilera, J., Hinks, M. L., Aiona, P. K., Wingen, L. M., Horne, J. R., Zhu, S., Dabdub, D., Laskin, A., Laskin, J., Lin, P., and Nizkorodov, S. A.: Reactive Uptake of Ammonia by Biogenic and Anthropogenic Organic Aerosols, in: Multiphase Environmental Chemistry in the Atmosphere, ACS Symposium Series, 1299, American Chemical Society, 127-147, doi:10.1021/bk-2018-1299.ch007

https://doi.org/10.5194/egusphere-2024-2602
Preprint. Discussion started: 7 October 2024

10.1021/bk-2018-1299.ch007, 2018.

Ng, N. L., Brown, S. S., Archibald, A. T., Atlas, E., Cohen, R. C., Crowley, J. N., Day, D. A., Donahue, N. M., Fry, J. L., Fuchs, H., Griffin, R. J., Guzman, M. I., Herrmann, H., Hodzic, A., Iinuma, Y., Jimenez, J. L., Kiendler-Scharr, A., Lee, B. H., Luecken, D. J., Mao, J., McLaren, R., Mutzel, A., Osthoff, H. D., Ouyang, B., Picquet-Varrault, B., Platt, U., Pye, H. O. T., Rudich, Y., Schwantes, R. H., Shiraiwa, M., Stutz, J., Thornton, J. A., Tilgner, A., Williams, B. J., and Zaveri, R. A.: Nitrate radicals and biogenic volatile organic compounds: oxidation, mechanisms, and organic aerosol, Atmos. Chem. Phys., 17, 2103-2162, 10.5194/acp-17-2103-2017, 2017.

Nguyen, T. B., Bates, K. H., Crounse, J. D., Schwantes, R. H., Zhang, X., Kjaergaard, H. G., Surratt, J. D., Lin, P., Laskin, A., Seinfeld, J. H., and Wennberg, P. O.: Mechanism of the hydroxyl radical oxidation of methacryloyl peroxynitrate (MPAN) and its pathway toward secondary organic aerosol formation in the atmosphere, Phys. Chem. Chem. Phys., 17, 17914-17926, https://doi.org/10.1039/C5CP02001H, 2015.

Nie, W., Yan, C., Huang, D. D., Wang, Z., Liu, Y., Qiao, X., Guo, Y., Tian, L., Zheng, P., Xu, Z., Li, Y., Xu, Z., Qi, X., Sun, P., Wang, J., Zheng, F., Li, X., Yin, R., Dallenbach, K. R., Bianchi, F., Petäjä, T., Zhang, Y., Wang, M., Schervish, M., Wang, S., Qiao, L., Wang, Q., Zhou, M., Wang, H., Yu, C., Yao, D., Guo, H., Ye, P., Lee, S.,

https://doi.org/10.5194/egusphere-2024-2602
Preprint. Discussion started: 7 October 2024

863 Li, Y. J., Liu, Y., Chi, X., Kerminen, V.-M., Ehn, M., Donahue, N. M., Wang, T.,
864 Huang, C., Kulmala, M., Worsnop, D., Jiang, J., and Ding, A.: Secondary organic
865 aerosol formed by condensing anthropogenic vapours over China's megacities, Nature
866 Geoscience, 15, 255-261, 10.1038/s41561-022-00922-5, 2022.

867 Oksanen, J., Kindt, R., Legendre, P., O'Hara, B., Stevens, M. H. H., Oksanen, M.
868 J., and Suggests, M.: The vegan package, Community ecology package, 10, 719, 2007.

869 Perraud, V., Bruns, E. A., Ezell, M. J., Johnson, S. N., Yu, Y., Alexander, M. L.,
870 Zelenyuk, A., Imre, D., Chang, W. L., Dabdub, D., Pankow, J. F., and Finlayson-Pitts,
871 B. J.: Nonequilibrium atmospheric secondary organic aerosol formation and growth, P.
872 Natl. Acad. Sci. USA, 109, 2836-2841, doi:10.1073/pnas.1119909109, 2012.

873 Rollins, A. W., Browne, E. C., Min, K.-E., Pusede, S. E., Wooldridge, P. J.,
874 Gentner, D. R., Goldstein, A. H., Liu, S., Day, D. A., Russell, L. M., and Cohen, R. C.:
875 Evidence for NO_x Control over Nighttime SOA Formation, Science, 337, 1210-1212,
876 https://doi.org/10.1126/science.1221520, 2012.

877 Shen, Z., Cao, J., Arimoto, R., Han, Z., Zhang, R., Han, Y., Liu, S., Okuda, T.,
878 Nakao, S., and Tanaka, S.: Ionic composition of TSP and PM2.5 during dust storms
879 and air pollution episodes at Xi'an, China, Atmos. Environ., 43, 2911-2918,
880 https://doi.org/10.1016/j.atmosenv.2009.03.005, 2009.

881 Shi, X., Qiu, X., Cheng, Z., Chen, Q., Rudich, Y., and Zhu, T.: Isomeric
882 Identification of Particle-Phase Organic Nitrates through Gas Chromatography and

https://doi.org/10.5194/egusphere-2024-2602
Preprint. Discussion started: 7 October 2024

Time-of-Flight Mass Spectrometry Coupled with an Electron Capture Negative Ionization Source, Environ. Sci. Technol., 54, 707-713, 10.1021/acs.est.9b05818, 2020.

Shi, X., Qiu, X., Li, A., Jiang, X., Wei, G., Zheng, Y., Chen, Q., Chen, S., Hu, M., Rudich, Y., and Zhu, T.: Polar Nitrated Aromatic Compounds in Urban Fine Particulate Matter: A Focus on Formation via an Aqueous-Phase Radical Mechanism, Environ. Sci. Technol., 57, 5160-5168, 10.1021/acs.est.2c07324, 2023.

Singh, S. and Kumar, R.: Air Pollution and Its Associated Impacts on Atmosphere and Biota Health, in: Extremes in Atmospheric Processes and Phenomenon: Assessment, Impacts and Mitigation, edited by: Saxena, P., Shukla, A., and Gupta, A. K., Springer Nature Singapore, Singapore, 29-58, 10.1007/978-981-16-7727-4_3, 2022.

Song, J., Li, M., Jiang, B., Wei, S., Fan, X., and Peng, P. a.: Molecular Characterization of Water-Soluble Humic like Substances in Smoke Particles Emitted from Combustion of Biomass Materials and Coal Using Ultrahigh-Resolution Electrospray Ionization Fourier Transform Ion Cyclotron Resonance Mass Spectrometry, Environ. Sci. Technol., 52, 2575-2585, https://doi.org/10.1021/acs.est.7b06126, 2018.

Song, J., Li, M., Zou, C., Cao, T., Fan, X., Jiang, B., Yu, Z., Jia, W., and Peng, P. a.: Molecular Characterization of Nitrogen-Containing Compounds in Humic-like

https://doi.org/10.5194/egusphere-2024-2602
Preprint. Discussion started: 7 October 2024

903 Substances Emitted from Biomass Burning and Coal Combustion, Environ. Sci.
904 Technol., 56, 119-130, https://doi.org/10.1021/acs.est.1c04451, 2022.
905 Stockwell, C. E., Veres, P. R., Williams, J., and Yokelson, R. J.: Characterization
906 of biomass burning emissions from cooking fires, peat, crop residue, and other fuels
907 with high-resolution proton-transfer-reaction time-of-flight mass spectrometry, Atmos.
908 Chem. Phys., 15, 845-865, 10.5194/acp-15-845-2015, 2015.
909 Streets, D. G. and Waldhoff, S. T.: Present and future emissions of air pollutants
910 in China:: SO2, NOx, and CO, Atmos. Environ., 34, 363-374,
911 https://doi.org/10.1016/S1352-2310(99)00167-3, 2000.
912 Su, S., Xie, Q., Lang, Y., Cao, D., Xu, Y., Chen, J., Chen, S., Hu, W., Qi, Y., Pan,
913 X., Sun, Y., Wang, Z., Liu, C.-Q., Jiang, G., and Fu, P.: High Molecular Diversity of
914 Organic Nitrogen in Urban Snow in North China, Environ. Sci. Technol., 55, 4344-
915 4356, https://dx.doi.org/10.1021/acs.est.0c06851, 2021.
916 Suess, E., Aemisegger, F., Sonke, J. E., Sprenger, M., Wernli, H., and Winkel, L.
917 H. E.: Marine versus Continental Sources of Iodine and Selenium in Rainfall at Two
918 European High-Altitude Locations, Environ. Sci. Technol., 53, 1905-1917,
919 10.1021/acs.est.8b05533, 2019.
920 Sun, W., Hu, X., Fu, Y., Zhang, G., Zhu, Y., Wang, X., Yan, C., Xue, L., Meng,
921 H., Jiang, B., Liao, Y., Wang, X., Peng, P., and Bi, X.: Different formation pathways
922 of nitrogen-containing organic compounds in aerosols and fog water in northern

https://doi.org/10.5194/egusphere-2024-2602
Preprint. Discussion started: 7 October 2024

China, Atmos. Chem. Phys., 24, 6987-6999, 10.5194/acp-24-6987-2024, 2024.

Surratt, J. D., Chan, A. W. H., Eddingsaas, N. C., Chan, M., Loza, C. L., Kwan, A. J., Hersey, S. P., Flagan, R. C., Wennberg, P. O., and Seinfeld, J. H.: Reactive intermediates revealed in secondary organic aerosol formation from isoprene, P. Natl. Acad. Sci. USA, 107, 6640-6645, doi:10.1073/pnas.0911114107, 2010.

Vione, D., Maurino, V., Minero, C., and Pelizzetti, E.: Aqueous Atmospheric Chemistry: Formation of 2,4-Dinitrophenol upon Nitration of 2-Nitrophenol and 4-Nitrophenol in Solution, Environ. Sci. Technol., 39, 7921-7931, 10.1021/es050824m, 2005.

Vu, T. V., Shi, Z., Cheng, J., Zhang, Q., He, K., Wang, S., and Harrison, R. M.: Assessing the impact of clean air action on air quality trends in Beijing using a machine learning technique, Atmos. Chem. Phys., 19, 11303-11314, 10.5194/acp-19-11303-2019, 2019.

Wang, D., Shen, Z., Yang, X., Huang, S., Luo, Y., Bai, G., and Cao, J.: Insight into the Role of NH3/NH4+ and NOx/NO3– in the Formation of Nitrogen-Containing Brown Carbon in Chinese Megacities, Environ. Sci. Technol., 58, 4281-4290, 10.1021/acs.est.3c10374, 2024.

Wang, J., Sun, S., Zhang, C., Xue, C., Liu, P., Zhang, C., Mu, Y., Wu, H., Wang, D., Chen, H., and Chen, J.: The pollution levels, variation characteristics, sources and implications of atmospheric carbonyls in a typical rural area of North China Plain

https://doi.org/10.5194/egusphere-2024-2602
Preprint. Discussion started: 7 October 2024

943 during winter, Journal of Environmental Sciences, 95, 256-265,
944 https://doi.org/10.1016/j.jes.2020.05.003, 2020.
945 Wang, J., Ye, J., Zhang, Q., Zhao, J., Wu, Y., Li, J., Liu, D., Li, W., Zhang, Y.,
946 Wu, C., Xie, C., Qin, Y., Lei, Y., Huang, X., Guo, J., Liu, P., Fu, P., Li, Y., Lee, H. C.,
947 Choi, H., Zhang, J., Liao, H., Chen, M., Sun, Y., Ge, X., Martin, S. T., and Jacob, D. J.:
948 Aqueous production of secondary organic aerosol from fossil-fuel emissions in winter
949 Beijing haze, P. Natl. Acad. Sci. USA, 118, e2022179118,
950 doi:10.1073/pnas.2022179118, 2021a.
951 Wang, K., Zhang, Y., Huang, R.-J., Cao, J., and Hoffmann, T.: UHPLC-Orbitrap
952 mass spectrometric characterization of organic aerosol from a central European city
953 (Mainz, Germany) and a Chinese megacity (Beijing), Atmos. Environ., 189, 22-29,
954 https://doi.org/10.1016/j.atmosenv.2018.06.036, 2018.
955 Wang, K., Huang, R.-J., Brueggemand, M., Zhang, Y., Yang, L., Ni, H., Guo, J.,
956 Wang, M., Han, J., Bilde, M., Glasius, M., and Hoffmann, T.: Urban organic aerosol
957 composition in eastern China differs from north to south: molecular insight from a
958 liquid chromatography-mass spectrometry (Orbitrap) study, Atmos. Chem. Phys., 21,
959 9089-9104, https://doi.org/10.5194/acp-21-9089-2021, 2021b.
960 Wang, Y., Zhao, Y., Li, Z., Li, C., Yan, N., and Xiao, H.: Importance of Hydroxyl
961 Radical Chemistry in Isoprene Suppression of Particle Formation from α-Pinene
962 Ozonolysis, ACS Earth Space Chem., 5, 487-499,

https://doi.org/10.5194/egusphere-2024-2602
Preprint. Discussion started: 7 October 2024

https://doi.org/10.1021/acsearthspacechem.0c00294, 2021c.

Wang, Y., Zhuang, G., Zhang, X., Huang, K., Xu, C., Tang, A., Chen, J., and An, Z.: The ion chemistry, seasonal cycle, and sources of PM2.5 and TSP aerosol in Shanghai, Atmos. Environ., 40, 2935-2952, https://doi.org/10.1016/j.atmosenv.2005.12.051, 2006.

Wang, Y., Hu, M., Lin, P., Guo, Q., Wu, Z., Li, M., Zeng, L., Song, Y., Zeng, L., Wu, Y., Guo, S., Huang, X., and He, L.: Molecular Characterization of Nitrogen-Containing Organic Compounds in Humic-like Substances Emitted from Straw Residue Burning, Environ. Sci. Technol., 51, 5951-5961, https://doi.org/10.1021/acs.est.7b00248, 2017.

Wang, Y., Hu, M., Hu, W., Zheng, J., Niu, H., Fang, X., Xu, N., Wu, Z., Guo, S., Wu, Y., Chen, W., Lu, S., Shao, M., Xie, S., Luo, B., and Zhang, Y.: Secondary Formation of Aerosols Under Typical High-Humidity Conditions in Wintertime Sichuan Basin, China: A Contrast to the North China Plain, J. Geophys. Res.-Atmos., 126, e2021JD034560, https://doi.org/10.1029/2021JD034560, 2021d.

Wen, W., Shi, L., Li, L., Wang, L., and Chen, J.: Molecular characteristics of ambient organic aerosols in Shanghai winter before and after the COVID-19 outbreak, Sci. Total Environ., 869, 161811, https://doi.org/10.1016/j.scitotenv.2023.161811, 2023.

Wu, Z., Wang, Y., Tan, T., Zhu, Y., Li, M., Shang, D., Wang, H., Lu, K., Guo, S.,

https://doi.org/10.5194/egusphere-2024-2602
Preprint. Discussion started: 7 October 2024

983 Zeng, L., and Zhang, Y.: Aerosol Liquid Water Driven by Anthropogenic Inorganic
984 Salts: Implying Its Key Role in Haze Formation over the North China Plain, Environ.
985 Sci. Technol. Lett., 5, 160-166, 10.1021/acs.estlett.8b00021, 2018.
986 Xi, Y., Wang, Q., Zhu, J., Yang, M., Hao, T., Chen, Y., Zhang, Q., He, N., and Yu,
987 G.: Atmospheric wet organic nitrogen deposition in China: Insights from the national
988 observation network, Sci. Total Environ., 898, 165629,
989 https://doi.org/10.1016/j.scitotenv.2023.165629, 2023.
990 Xiao, H.-Y. and Liu, C.-Q.: Chemical characteristics of water-soluble
991 components in TSP over Guiyang, SW China, 2003, Atmos. Environ., 38, 6297-6306,
992 https://doi.org/10.1016/j.atmosenv.2004.08.033, 2004.
993 Xu, B., Zhang, G., Gustafsson, Ö., Kawamura, K., Li, J., Andersson, A., Bikkina,
994 S., Kunwar, B., Pokhrel, A., Zhong, G., Zhao, S., Li, J., Huang, C., Cheng, Z., Zhu, S.,
995 Peng, P., and Sheng, G.: Large contribution of fossil-derived components to aqueous
996 secondary organic aerosols in China, Nature Communications, 13, 5115,
997 10.1038/s41467-022-32863-3, 2022a.
998 Xu, Y., Xiao, H., Wu, D., and Long, C.: Abiotic and Biological Degradation of
999 Atmospheric Proteinaceous Matter Can Contribute Significantly to Dissolved Amino
1000 Acids in Wet Deposition, Environ. Sci. Technol., 54, 6551-6561,
1001 10.1021/acs.est.0c00421, 2020a.
1002 Xu, Y., Dong, X.-N., Xiao, H.-Y., He, C., and Wu, D.-S.: Water-Insoluble

https://doi.org/10.5194/egusphere-2024-2602
Preprint. Discussion started: 7 October 2024

Components in Rainwater in Suburban Guiyang, Southwestern China: A Potential Contributor to Dissolved Organic Carbon, J. Geophys. Res.-Atmos., 127, e2022JD037721, https://doi.org/10.1029/2022JD037721, 2022b.

Xu, Y., Dong, X.-N., Xiao, H.-Y., Zhou, J.-X., and Wu, D.-S.: Proteinaceous Matter and Liquid Water in Fine Aerosols in Nanchang, Eastern China: Seasonal Variations, Sources, and Potential Connections, J. Geophys. Res.-Atmos., 127, e2022JD036589, https://doi.org/10.1029/2022JD036589, 2022c.

Xu, Y., Dong, X. N., He, C., Wu, D. S., Xiao, H. W., and Xiao, H. Y.: Mist cannon trucks can exacerbate the formation of water-soluble organic aerosol and $PM_{2.5}$ pollution in the road environment, Atmos. Chem. Phys., 23, 6775-6788, https://doi.org/10.5194/acp-23-6775-2023, 2023.

Xu, Y., Liu, T., Ma, Y. J., Sun, Q. B., Xiao, H. W., Xiao, H., and Xiao, H. Y.: Measurement report: Characteristics of aminiums in PM2.5 during winter clean and polluted episodes in China: aminium outbreak and its constraint, EGUsphere, 2024, 1-36, 10.5194/egusphere-2024-975, 2024.

Xu, Y., Miyazaki, Y., Tachibana, E., Sato, K., Ramasamy, S., Mochizuki, T., Sadanaga, Y., Nakashima, Y., Sakamoto, Y., Matsuda, K., and Kajii, Y.: Aerosol Liquid Water Promotes the Formation of Water-Soluble Organic Nitrogen in Submicrometer Aerosols in a Suburban Forest, Environ. Sci. Technol., 54, 1406-1414, https://dx.doi.org/10.1021/acs.est.9b05849, 2020b.

https://doi.org/10.5194/egusphere-2024-2602
Preprint. Discussion started: 7 October 2024

Yang, L., Huang, R.-J., Yuan, W., Huang, D. D., and Huang, C.: pH-Dependent Aqueous-Phase Brown Carbon Formation: Rate Constants and Implications for Solar Absorption and Atmospheric Photochemistry, Environ. Sci. Technol., 58, 1236-1243, 10.1021/acs.est.3c07631, 2024a.

Yang, T., Xu, Y., Ma, Y.-J., Wang, Y.-C., Yu, J. Z., Sun, Q.-B., Xiao, H.-W., Xiao, H.-Y., and Liu, C.-Q.: Field Evidence for Constraints of Nearly Dry and Weakly Acidic Aerosol Conditions on the Formation of Organosulfates, Environ. Sci. Technol. Lett., 11, 981-987, 10.1021/acs.estlett.4c00522, 2024b.

Yang, T., Xu, Y., Ye, Q., Ma, Y. J., Wang, Y. C., Yu, J. Z., Duan, Y. S., Li, C. X., Xiao, H. W., Li, Z. Y., Zhao, Y., and Xiao, H. Y.: Spatial and diurnal variations of aerosol organosulfates in summertime Shanghai, China: potential influence of photochemical processes and anthropogenic sulfate pollution, Atmos. Chem. Phys., 23, 13433-13450, https://doi.org/10.5194/acp-23-13433-2023, 2023.

Yassine, M. M., Harir, M., Dabek-Zlotorzynska, E., and Schmitt-Kopplin, P.: Structural characterization of organic aerosol using Fourier transform ion cyclotron resonance mass spectrometry: Aromaticity equivalent approach, Rapid Commun. Mass Spectrom., 28, 2445-2454, https://doi.org/10.1002/rcm.7038, 2014.

Yu, X., Pan, Y., Song, W., Li, S., Li, D., Zhu, M., Zhou, H., Zhang, Y., Li, D., Yu, J., Wang, X., and Wang, X.: Wet and Dry Nitrogen Depositions in the Pearl River Delta, South China: Observations at Three Typical Sites With an Emphasis on Water-

https://doi.org/10.5194/egusphere-2024-2602
Preprint. Discussion started: 7 October 2024

Soluble Organic Nitrogen, J. Geophys. Res.-Atmos., 125, e2019JD030983, https://doi.org/10.1029/2019JD030983, 2020.

Yuan, W., Huang, R.-J., Shen, J., Wang, K., Yang, L., Wang, T., Gong, Y., Cao, W., Guo, J., Ni, H., Duan, J., and Hoffmann, T.: More water-soluble brown carbon after the residential "coal-to-gas" conversion measure in urban Beijing, npj Climate and Atmospheric Science, 6, 20, 10.1038/s41612-023-00355-w, 2023.

Zeng, Y., Ning, Y., Shen, Z., Zhang, L., Zhang, T., Lei, Y., Zhang, Q., Li, G., Xu, H., Ho, S. S. H., and Cao, J.: The Roles of N, S, and O in Molecular Absorption Features of Brown Carbon in PM2.5 in a Typical Semi-Arid Megacity in Northwestern China, J. Geophys. Res.-Atmos., 126, e2021JD034791, https://doi.org/10.1029/2021JD034791, 2021.

Zhang, B., Shen, Z., He, K., Zhang, L., Huang, S., Sun, J., Xu, H., Li, J., Yang, L., and Cao, J.: Source Profiles of Particle-Bound Phenolic Compounds and Aromatic Acids From Fresh and Aged Solid Fuel Combustion: Implication for the Aging Mechanism and Newly Proposed Source Tracers, J. Geophys. Res.-Atmos., 128, e2023JD039758, https://doi.org/10.1029/2023JD039758, 2023a.

Zhang, H., He, P., Liu, L., Dai, H., Zhao, B., Zeng, Y., Bi, J., Liu, M., and Ji, J. S.: Trade-offs between cold protection and air pollution–induced mortality of China's heating policy, PNAS Nexus, 2, 10.1093/pnasnexus/pgad387, 2023b.

Zhang, T., Cao, J. J., Tie, X. X., Shen, Z. X., Liu, S. X., Ding, H., Han, Y. M.,

https://doi.org/10.5194/egusphere-2024-2602
Preprint. Discussion started: 7 October 2024

1063 Wang, G. H., Ho, K. F., Qiang, J., and Li, W. T.: Water-soluble ions in atmospheric
1064 aerosols measured in Xi'an, China: Seasonal variations and sources, Atmos. Res., 102,
1065 110-119, https://doi.org/10.1016/j.atmosres.2011.06.014, 2011.
1066 Zhang, Y.-L. and Cao, F.: Fine particulate matter (PM2.5) in China at a city level,
1067 Scientific Reports, 5, 14884, 10.1038/srep14884, 2015.
1068 Zhang, Z., Guan, H., Xiao, H., Liang, Y., Zheng, N., Luo, L., Liu, C., Fang, X.,
1069 and Xiao, H.: Oxidation and sources of atmospheric NOx during winter in Beijing
1070 based on δ18O-δ15N space of particulate nitrate, Environmental Pollution, 276,
1071 116708, https://doi.org/10.1016/j.envpol.2021.116708, 2021a.
1072 Zhang, Z., Zhou, Y., Zhao, N., Li, H., Tohniyaz, B., Mperejekumana, P., Hong,
1073 Q., Wu, R., Li, G., Sultan, M., Zayan, A. M. I., Cao, J., Ahmad, R., and Dong, R.:
1074 Clean heating during winter season in Northern China: A review, Renewable and
1075 Sustainable Energy Reviews, 149, 111339, https://doi.org/10.1016/j.rser.2021.111339,
1076 2021b.
1077 Zhao, D. and Sun, B.: Atmospheric Pollution from Coal Combustion in China,
1078 Journal of the Air Pollution Control Association, 36, 371-374,
1079 10.1080/00022470.1986.10466074, 1986.
1080